12-2014

Thermo-physical Property Models and Effect on Heat Pipe Modelling

Devakar Dhingra
Clemson University, ddhingr@g.clemson.edu

Recommended Citation

Dhingra, Devakar, "Thermo-physical Property Models and Effect on Heat Pipe Modelling" (2014). *All Theses*. 2052.
https://tigerprints.clemson.edu/all_theses/2052

THERMO-PHYSICAL PROPERTY MODELS

AND

EFFECT ON HEAT PIPE MODELING

A Thesis
Presented to
the Graduate School of
Clemson University

In Partial Fulfillment
of the Requirements for the Degree
Master of Science
Mechanical Engineering

---

by
Devakar Dhingra
November 2014

Accepted by:
Dr. Jay M. Ochterbeck, Committee Chair & Advisor
Dr. Xiangchun Xuan, Committee member
Dr. Chenning Tong, Committee member

ABSTRACT

Heat transfer devices find applications in various aspects of life. Be it residential, commercial or industrial application, efficient heat transfer is a challenge to all. Other than geometric design considerations and wick selection, the optimization of heat transfer in the heat pipe also depends on fluid selection. Heat pipe technology has proven to work efficiently with properly selected thermal fluid, from cryogenic temperatures to very high temperatures. Higher heat transfer ability through small temperature differences makes the heat pipe an efficient technology. Hence, it can be stated that selecting a proper working fluid enhances the heat transfer performance of a heat pipe. For selecting the working fluid, important thermo-physical properties to be considered are density, viscosity, surface tension, latent heat of vaporization and vapor saturation pressure at every working temperature.

The operating range of the working fluid starts from the triple point and till the critical point. The performance of the working fluid is not optimum at both ends of the operating range of temperature. At critical temperature, it is impacted by low surface tension and latent heat of vaporization, whereas near the triple point low vapor density and high viscosity affects the performance.

One of the first indices for evaluating the performance of the working fluid is called “Merit Number” This merit number considers a single pressure gradient, i.e. the liquid pressure drop. Later, substantial works have been done to implement the same idea in a system utilizing multiple pressure gradients (losses). In all the methods comparing the merit number of the fluids, the higher the merit number, better is the heat transfer capacity of the pipe.

For theoretical calculations and geometrical design considerations, thermo-physical property data of the working fluid at every operating temperature is not available and if available, the reliability of this data is a reason of concern. The present work constitutes of dividing the working fluids into two main categories polar fluids (i.e. ammonia, water and methanol) and nonpolar fluids (i.e. ethane) and thus validating the methods used for formulating these thermo-physical properties as a function of temperature.

As per conventional available data (in several reliable resources), these thermo-physical properties are formulated as a polynomial function of the temperature. The main problem though with such formulation is the data reliability outside the specified temperature range. This work tries to formulate such properties as a function of intensive properties and molecular structure of the working fluid. Thereafter the most useful method for thermo-physical property formulation was chosen after calculating the error percentage (relating to the experimental data obtained from various sources)

The latter part of this work focuses on the uncertainty of the value about the mean obtained from the methods used and thereafter the percent deviation (between the mean obtained and the experimental data available) which can give the clear idea about the selection of the method for formulating the properties.

The last part of this work link the different methods used with the merit number for both liquid and vapor driven heat pipe. This part also includes the error percent and deviation percentage of the capillary limited maximum heat transferring capacity of the heat pipe.

DEDICATION

This work is dedicated to my family and friends whose unconditional support, love and belief in me, encouraged me in every shape of life.

ACKNOWLEDGEMENT

I would like to express my sincere gratitude to my advisor Dr. Jay M. Ochterbeck for his continued and extensive support and relevant feedback throughout the work.

TABLE OF CONTENTS

Page

CHAPTER 1

CHAPTER 2

CHAPTER 3

Table of contents (Continued)

Page

CHAPTER 4

CHAPTER 5

LIST OF TABLES

Table Page

List of Tables (Continued)

LIST OF FIGURES

List of Figures (Continued)

Figure Page

NOMENCLATURE

A	Area (Cross-sectional)
F.m	Merit Number (W/m^2)
f	Frictional Factor
K	Boltzmann Constant.
k	Wick Permeability
l	Length
M	Molecular Mass (g/mole)
P	Pressure
p	Dipole Moment (debyes)
Q	Heat (W)
R	Gas Constant (8.314 j/ (mole K))
r	Radius
Re	Reynolds Number
T	Temperature
V	Volume
v	Specific Volume (cm3\mole)
Z	Compressibility Factor
ε	Porosity
γ	Molecular Potential Energy
λ	Latent Heat of vaporization
μ	Dynamic Viscosity
ρ	Density
σ	Surface Tension
θ	Angle of Inclination
ω	Acentric Factor
$\ni$	Collision Integral

Subscripts

b	Boiling
c	Critical
ca	Capillary
cond	Condenser
eff	Effective
evap	Evaporator
g	Groove
h	Hydraulic
k	Known Parameter
l	Liquid
lam	Laminar
lhp	Loop Heat Pipe
Mol	Molar Volume (cm3/mole)
m	Maximum

Nomenclature (Continued)

p	Pore
r	Reduced
s	Saturation
turb	Turbulence
v	Vapor
vl	Vapor-Liquid
w	Wick

CHAPTER 1

INTRODUCTION

Heat pipe is a highly efficient heat transfer mechanism, which works upon the evaporation and the condensation cycle of the thermal fluid [1]. The latent heat of vaporization is absorbed by the working fluid at the evaporator section, which starts the heat transfer mechanism by reducing the temperature at the hot evaporator end, after which the heat is transported towards the condenser end where it is rejected out.

Conventional Heat Pipe

In its simplest form, a conventional heat pipe is a closed cylinder, consisting of three main sections: the evaporator, the condenser and the adiabatic transport section as shown in Fig. 1. The porous wick that runs throughout the cylindrical casing is always saturated with working fluid if the heat pipe is operating correctly.

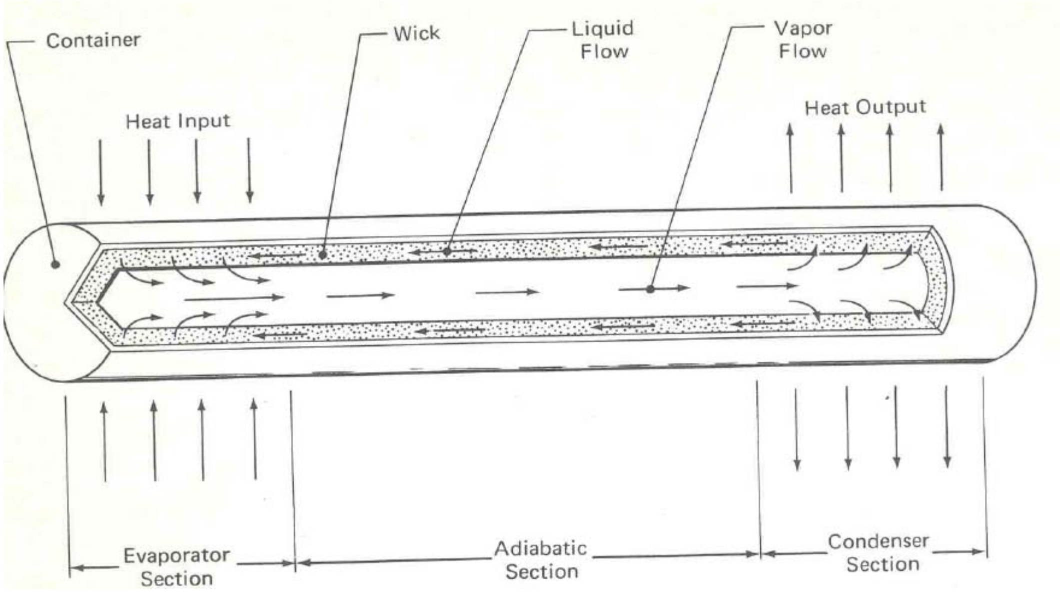

Figure 1: Conventional heat pipe [1]

These sections are usually defined by the thermal boundary conditions, as the internal section is typically uniform [2]. The evaporator section is exposed to the heat source, once the heat is conducted through the casing and into the wick, the fluid vaporizes and flows through the adiabatic section to the condenser section and finally the vapor is condensed in the condenser section. The capillary forces thus developed in the porous wick, pumps the condensed liquid back to the evaporator [1]. The closed cylinder container should be thermally and chemically stable (non-reactive to the working fluid even at high temperature and pressures) and should have good thermal conductivity. The purpose of the wick defined in [3] is to provide:

1. The necessary flow passage for the returning fluid.
2. Development of the required capillary pressure
3. A heat flow path between the inner wall and the working fluid.

During the steady state operation of the heat pipe, when the fluid, in the form of the vapor flows from evaporator to condenser, there exists a vapor pressure gradient ($\triangle P_v$) along its flow. After condensation, when the liquid returns to the evaporator, there exists a liquid pressure gradient ($\triangle P_l$). For the continuous operation, the maximum pressure or the capillary pressure (Eq. 1) must exceed all the other pressure gradients (Eq. 2) at all times.

$$\Delta P_{ca} = 2 * \frac{\sigma}{r_{ca}} * \cos(\theta) \tag{1}$$

$$\Delta P_{ca} \geq \Delta P_l + \Delta P_v + \Delta P_g \tag{2}$$

Hydrostatic pressure loss (Δ P_g) depends upon the orientation of the heat pipe. When the condenser is elevated above the evaporator, the gravity helps the fluid to return to the evaporator. But, when the evaporator is elevated above the condenser then the capillary forces has to overcome the hydrostatic pressure losses [1].

The maximum heat transport capability depends upon the limitations of the heat pipe. There are five major heat pipe limitations which constraints the circulation of the working fluid.

- Viscous Limit: At low temperature, or especially the starting of the heat pipe, the vapor pressure drop thus developed is not sufficient to overcome the high viscous forces. Thus, vapor from the evaporator does not start to flow and the circulation cycle doesn’t initiate.
- Sonic Limit: When the vapor velocity in the evaporator reaches sonic velocity it results in a chocked flow. This also constraints the circulation cycle of the working fluid.
- Capillary Limit: The wick generates capillary pressure to pump the condensed liquid back to the evaporator. When the capillary pressure developed is too low to pump the liquid to the evaporator, it leads to the dry out in the evaporator and the fluid circulation cycle stops.
- Entrainment limit: The high vapor concentration at the condenser end can lead to hinder the return flow to evaporator. Under such circumstances also there is pressure dry out in the evaporator and circulation stops.
- Boiling Limit: At high temperature, the temperature increased by high evaporator heat flux sometimes exceeds the degree of superheat. This

condition is the onset for the nucleate boiling of the fluid, which again causes dry out in the evaporator

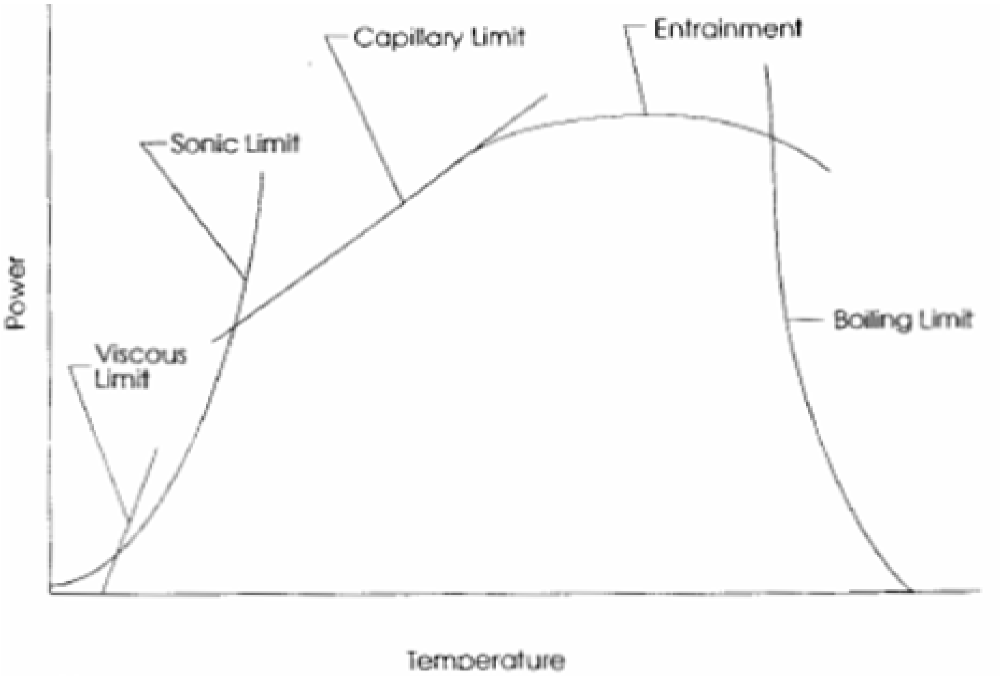

Figure 2: Heat Pipe Limitations [1]

Each limit plays an important role in its specified region of operating temperature. Viscous limit and sonic limit occurs at lower temperature, whereas entrainment limit and boiling limit are caused at high operating temperatures. Capillary limit is the most important amongst all and is responsible for defining the maximum heat transport capacity of the heat pipe for the majority of given geometric specifications. Boiling limit is typically responsible for setting the maximum operating temperature of the heat pipe.

Loop Heat Pipe

Loop heat pipe (Fig. 3) is also a heat transfer device whose operating principle is based on the same principle as the conventional heat pipe. The special design and property of the capillary structure of the loop heat pipe is capable of transferring heat efficiently for distance up to several meters at all orientation in the gravity field and even further when place horizontally [4].

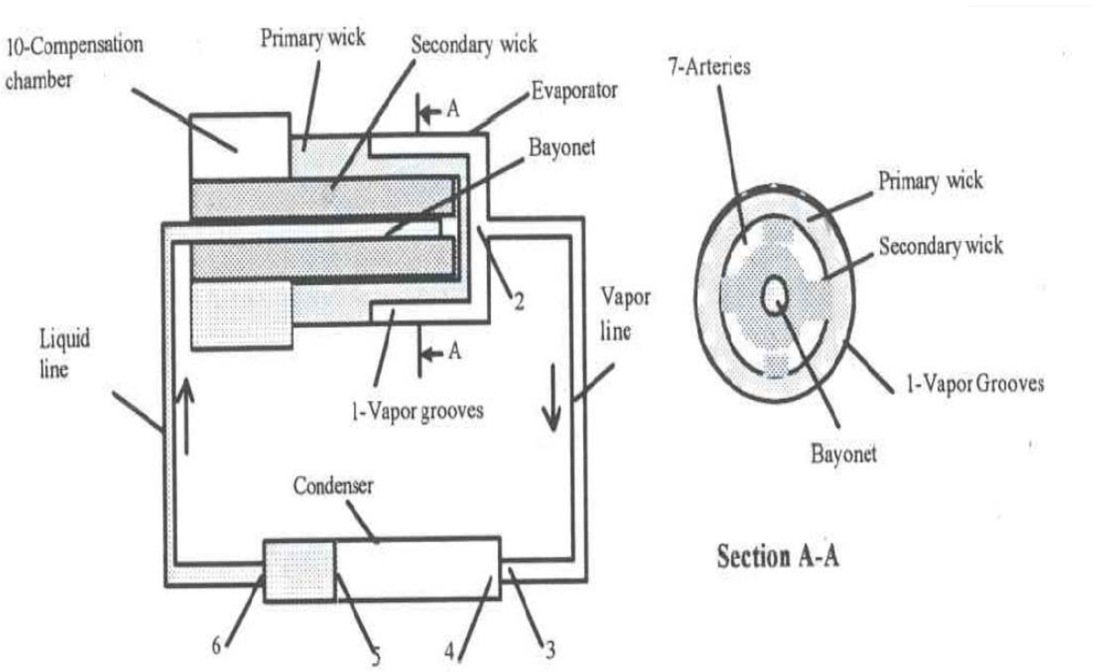

Figure 3: Loop heat pipe [5]

The key components of the loop heat pipe are evaporator, condenser, compensation chamber and liquid/vapor line [2]. The secondary wick (Fig. 3) maintains the proper supply of the working fluid to the evaporator. Whereas, the wick in the evaporator main section is known as the primary wick, is made of extremely fine pores for the purpose of developing high capillary pressures [4]. The secondary wick has larger pores than the primary wick, as its main function is to connect the compensation chamber and the evaporator. For the loop heat pipe, a pressure-temperature diagram of the fluid circulation is given in Fig. 4.

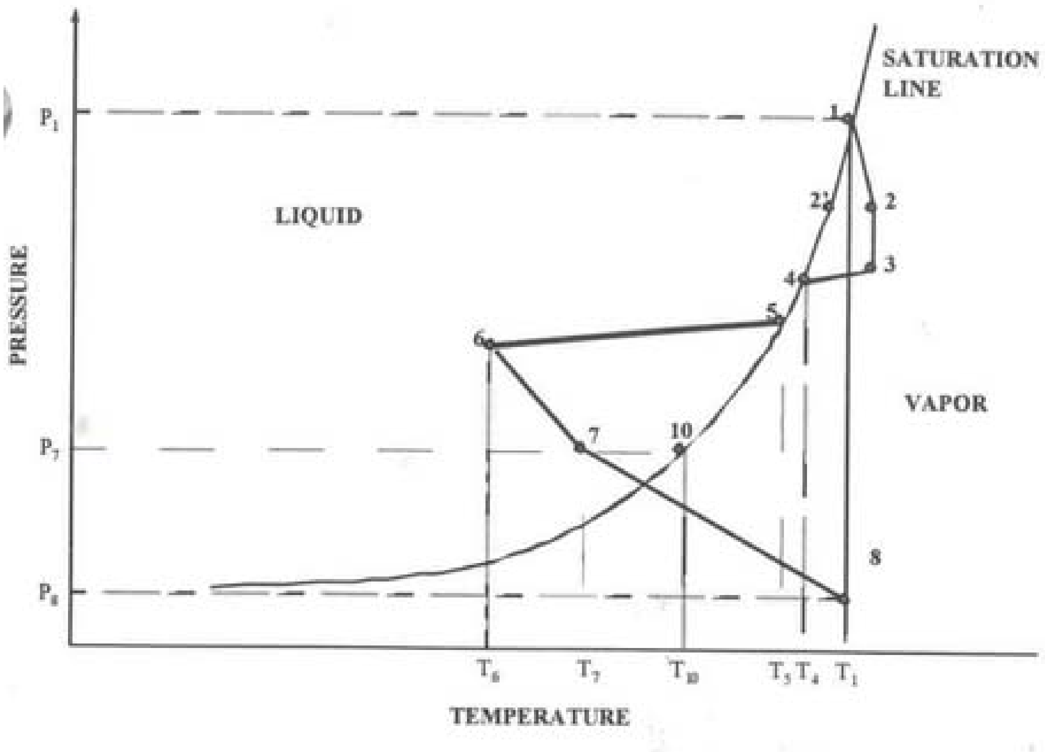

Figure 4: P-T diagram for LHP [5].

Fig. 4 shows the pressure vs temperature curve of the loop heat pipe working under steady state. The numbers in the figure corresponds to the geometric locations in the loop heat pipe as shown in Fig. 3. When the evaporator of the loop heat pipe comes in contact with the heat source, the liquid in the evaporator vaporizes and the fluid vapors are generated in the vapor grooves (point 1). Vapor at the evaporator exit (mainly the vapor groove) becomes super-heated due to decrease in pressure (point 2). The section from point 2 to point 3 represents the vapor flow in the vapor line assuming vapor line to be perfectly insulated, which should be ideally considered as isothermal [4].The cooling of the vapor take place at points 4, 5 and 6. Starting at point 4 and ending at point 5, the vapor losses its sensible heat and starts to condensate along the saturation curve. Liquid continues to be sub cooled between point 5 and 6. The sub cooled liquid flows in the liquid line and reaches the evaporator core (point 7). Since there is no flow between compensation chamber and evaporator core during the steady state operation, the pressure at the evaporator core (point 7) and that of the compensation chamber (point 10) must be equal [5]. Point 10 shows higher temperature due to the heat leak form evaporator core to the compensation chamber through the secondary wick.

The maximum operating pressure for the LHP is the capillary pressure (Eq. 1). The extremely small pore of the primary wick develops a high capillary pressure and thereby increases its maximum heat transport capacity. The maximum capillary pressure generated must be greater that all other pressure losses together. The pressure balance equation of the LHP can be seen in Eq.3 [2].

$$\Delta P_{ca} = 2 * \frac{\sigma}{r_{ca}} \geq \Delta P_{evap} + \Delta P_{v} + \Delta P_{cond} + \Delta P_{l} + \Delta P_{g} \qquad (3)$$

CHAPTER 2

LITERATURE REVIEW

Merit Number

The working fluid should have the melting temperature below the operating temperature range and the critical temperature above the operating temperature range. If the operating temperature is very high (i.e. approaching the critical temperature), the vapor will not condense and if it is too low (i.e. approaching the melting temperature), the liquid will not evaporate properly. Table. 1 shows the melting temperature, the boiling temperature, the critical temperature and the optimum working temperature range of some commonly used working fluids.

Fluid	Melting Temperature(K)	Boiling Temperature (k)	Critical Temperature (k)	Working Range (k)
Ammonia	195.4	240.0	405.5	220-370
Butane	134.8	272.6	425.1	140-360
Ethane	89.9	184.6	305.5	150-260
Ethanol	158.6	351.5	516.2	190-390
Heptane	182.6	371.6	540.2	250-420
Methanol	176.0	337.8	513.0	280-390
Toluene	178.1	383.8	593	190-450
Water	273.1	373.1	647	300-500

Table 1: Working fluid temperature table (at 1 atm) [34]

Since some fluids (Table.1) have over-lapping operating temperature ranges, a method is required for selecting the most desirable working fluid. The comparison indices given by S.W. Chi [1] is based on the heat pipe theory and is called as “Liquid Transport Factor” or “Merit Number”.

Chi developed a parameter for selecting the working fluid for conventional heat pipes using only the important thermo-physical properties of the fluids. This parameter compares the merits of the working fluid over the entire operating temperature. For a cylindrical heat pipe with uniform evaporator heat flux, the merit number is given by Eq. 4. There are six assumptions considered by Chi [1] for deriving the liquid merit number.

1) The pipe is capillary limited.
2) The vapor pressure losses are negligible.
3) Heat flux density is uniform at the evaporator and condenser section.
4) The heat pipe is operating in zero gravity field.
5) Fluid flow is laminar.
6) Capillaries are properly wetted

$$\mathrm{F.m_l} = \frac{\rho_l * \sigma * \lambda}{\mu_l} \tag{4}$$

According to the heat pipe theory [1], pressure losses in the system is dominated only by the liquid pressure drop (Eq. 5). The second parenthesis represents

$$\Delta P_l = \left(\frac{\mu_l}{\rho_l * \lambda}\right) * \left(\frac{f_l * Re}{2 * r_h^2}\right) * \left(\frac{Q * l_w}{A_w}\right) \tag{5}$$

the wick property. The hydraulic radius (r_h) is defined as the ratio of wick cross-sectional area to the wetted perimeter. For circular or cylindrical geometry, the hydraulic radius is considered to be capillary pore radius [1] and $f_l * Re = 16$ [7]. The maximum heat transport capacity (Eq. 6) of the liquid pressure gradient driven heat pipe depends on 3 factors (i) the fluid properties (ii) the wick property (wick permeability) and (iii) the wick geometry. The fluid properties (given in the first parenthesis of Eq. 5) were collectively called as the Liquid Transport Number by Chi or the Merit Number. Therefore by rearranging the terms (Eq. 5) it became clear that for designing the heat pipe, fluid selection plays an important role.

$$Q_m = 2 * \left(\frac{\rho_l * \sigma * \lambda}{\mu_l}\right) * \left(\frac{K}{r_{ca}}\right) * \left(\frac{A_w}{l_w}\right) \tag{6}$$

For a given fluid, the liquid merit number is a temperature dependent parameter which loses its significance at or near the critical temperature (see Fig. 5). The importance of the boiling temperature with respect to merit number was first studied by Asselman et al. [8]. Merit number for most working fluids, starts to increase from the triple point to a maximum around or after its normal boiling point, then decreases gradually, and vanishes near the critical temperature. Merit number for some fluids has been calculated at their respective normal boiling point (Table 2). A definite trend was observed relating higher merit number for the fluids having higher boiling temperature.

Asselman et al. [8] determined the merit number for the system in which liquid and gravitational pressure losses dominate the fluid flow. The maximum heat transport factor (Eq. 7) is again a function of three factors, the first parenthesis represents the wick geometry, the second parenthesis represents the orientation of heat pipe together with the wick property and the third parenthesis represents the working fluid property known as merit number. In the operating temperature range, the working fluid with highest merit number is selected for the optimum performance of the heat pipe.

$$Q_m = \left(\frac{4 * A_w * r_{ca}}{(f_l * Re) * l_w}\right) * \left(1 - \frac{\rho_l * g * l_w * \sin\theta * r_{ca}}{2 * \sigma}\right) * \left(\frac{\rho_l * \sigma * \lambda}{\mu_l}\right) \tag{7}$$

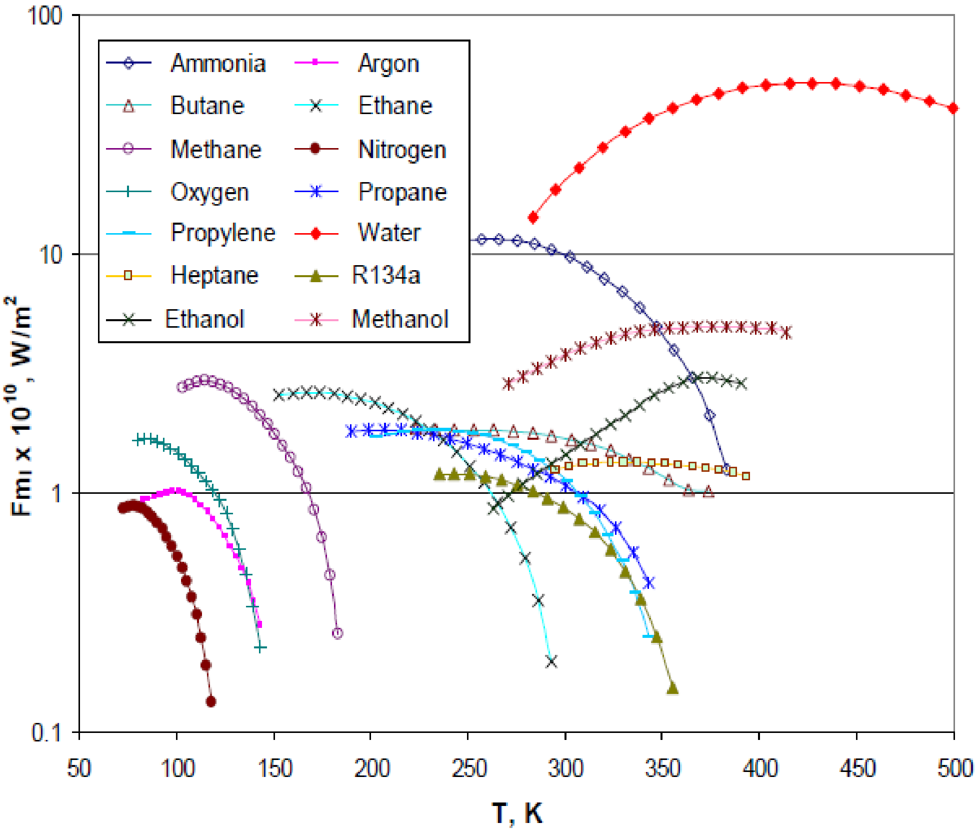

Figure 5: Liquid Merit number for different working fluids [9]

Fluid	T_m (k)	T_b (k)	ρ_l (kg/m^3)	μ_l (Pa-s)	σ (N/m)	λ (j/kg)	F.m (W/m^2)
Propene	88.0	225.6	608.4	$129*10^{-6}$	$5.9*10^{-3}$	$431*10^{3}$	$11.9*10^{9}$
Ammonia	194.9	240.0	681.4	$273*10^{-6}$	$33.9*10^{-3}$	$1369*10^{3}$	$11.5*10^{10}$
Butane	136 .0	273.0	604	$209*10^{-6}$	$15.4*10^{-3}$	$326.2*10^{3}$	$14.5*10^{9}$
Methanol	176.0	337.8	750.4	$300*10^{-6}$	$18.8-10^{-3}$	$1120*10^{3}$	$52.6*10^{9}$
Ethanol	159.0	351.5	757	$432*10^{-6}$	$17.3*10^{-3}$	$960*10^{3}$	$29.1*10^{9}$
Water	273.1	373.1	958.8	$279*10^{-6}$	$58.9*10^{-3}$	$2251*10^{3}$	$45.5*10^{10}$
Toluene	178.1	383.8	779.6	$247*10-^{6}$	$18.0*10-^{3}$	$370.5*10^{3}$	$21.0*10^{9}$

Table 2: Thermodynamic properties of several working fluids and merit number (at normal boiling temperature) [34]

Dunbar and Cadell [10] studied the heat pipe in which capillary pressure is only balanced by vapor pressure losses. The vapor pressure drop, given by Dunbar and Cadell (Eq. 8), which assumes very small vapor diameter lines and proper wick wetting. For zero gravity operation, the hydrostatic pressure loss is neglected. The maximum heat transport factor equation given by Dunbar and Cadell is shown in Eq. 9 and the vapor merit number is given in Eq. 10.

$$\mathrm{\Delta P_v} = 0.24 * \mathrm{l_{eff}} * \left(\frac{\mathrm{Q}}{\lambda}\right)^{1.75} * (2 * \mathrm{r_v})^{-4.75} * (\mu_v^{0.25}) * \left((\rho_v^{-1})\right) \tag{8}$$

$$2 * \frac{\sigma}{\mathrm{r_{ca}}} = 0.24 * \mathrm{l_{eff}} * \left(\frac{\mathrm{Q}}{\lambda}\right)^{1.75} * (2 * \mathrm{r_v})^{-4.75} * (\mu_v^{0.25}) * \left((\rho_v^{-1})\right) \tag{9}$$

$$\mathrm{F.m_v} = \frac{\sigma}{\lambda^{-1.75} * \ \mu_v^{0.25} * \ \rho_v^{-1}} \tag{10}$$

For a Loop heat pipe, the complex geometry (Fig. 6) of the evaporator section makes it challenging to support the fact that the vapor pressure losses are the only dominant losses. According to Mishkinis et al. [9], in some practical application the evaporator wick pressure loss is even higher than the vapor pressure loss. Changing some geometric parameters, such as reducing the length of the liquid line, increasing wick thickness or decreasing the effective pore radius can lead to dominating liquid pressure losses or wick pressure losses. Therefore, none of the previously mentioned merit number would hold true for such complex geometry alone.

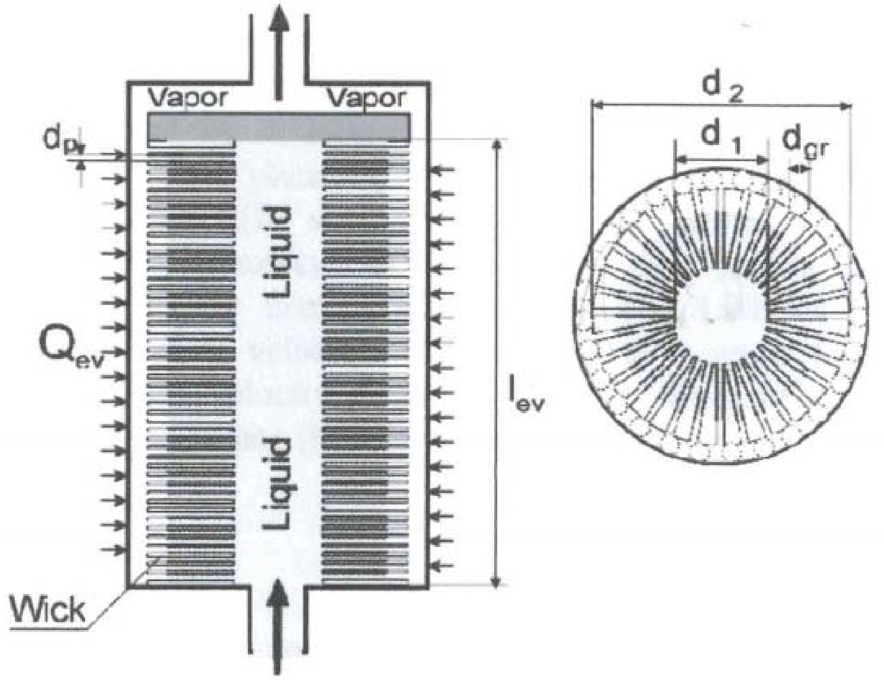

Figure 6: LHP Evaporator. [9]

The pressure balance equation (Eq. 11) for the loop heat pipe was formulated in [9]. Vapor flow in vapor line is turbulent, whereas liquid flow is laminar in the liquid line.

$$2\left(\frac{\sigma}{r_p}\right)\cos(\theta) = f_{turb}\rho_v V_v^2\left(\frac{l_{lhp}}{2 * d_v}\right) + 16V_w\mu_l\left(\frac{d_2 - d_1}{d_p^2}\right) + 32V_l\mu_l\left(\frac{l_{lhp}}{d_l^2}\right) \qquad (11)$$

First term describes the creation of the capillary head accounting for the maximum heat transport. The angle of inclination is added to include the gravity effect for the capillary suction pressure. The second term gives the vapor pressure loss with turbulent friction factor taken between 0.07-0.007 [9]. The turbulent friction factor taken was constant and don't depend upon the geometry of the loop heat pipe. The vapor velocity V_v (Eq. 12) can be derived by introducing the latent heat of vaporization and coupling it with mass conservation equation.

$$V_v = \frac{4 * Q}{\pi * h_{vl} * \rho_v * d_v^2} \tag{12}$$

The third term (Eq. 11) denotes the wick pressure losses. The wick velocity, often described by Darcy as seepage velocity is a complex parameter to define. Hence it is important to average the wick velocity over the entire seepage area. The wick velocity in integral form and the actual profile equation is given in Eq. 13.

$$V_w = \frac{\int_{\frac{d_1}{2}}^{\frac{d_2}{2}} V_w(r) * r\, dr}{\int_{\frac{d_1}{2}}^{\frac{d_2}{2}} r\, dr} = \frac{2 * Q}{\pi * \lambda_{fg} * \rho_l * \varepsilon * l_w * (d_2 + d_1)} \tag{13}$$

The liquid velocity (Eq. 14) is calculated in the same way the vapor velocity is calculated.

$$V_l = \frac{4 * Q}{\pi * \rho_l * \lambda_{vl} * d_l^2} \tag{14}$$

The pressure losses which are not considered to have a significant effect on the maximum heat transport capacity of the loop heat pipe occurs in evaporator vapor grooves, condenser section and compensation chamber. The above pressure balance equation (Eq.11) contains a second order heat transfer equation for maximum heat flux. The one positive root for heat transfer gives the vapor-liquid merit number for the working fluid selection. This approach directly depends upon the geometry of the evaporator of loop heat pipe as well as all the important thermo-physical properties of the working fluid. Therefore enclosing the geometry with all the important thermo-physical properties like viscosity, surface tension, density and latent heat, gives a better understanding of working fluid selection for loop heat pipe. Mishkinis et al. [9] solution for the vapor-liquid merit number is given in Eq. 15, taking f_{turb} as 0.0385.

$$\mathrm{F.m_{vl}} = \frac{((2.55\mathrm{K_l})^2 + 0.031\mathrm{K_v})^{0.5} - 2.55\mathrm{K_l}}{0.016\mathrm{K_v}} \tag{15}$$

Where,

$$\mathrm{K_l} = \frac{\mathrm{Geo_l}}{\mathrm{Fm_{l*}}} \qquad \mathrm{K_v} = \frac{\mathrm{Geo_v}}{\mathrm{Fm_{v*}}}$$

$$\mathrm{Geo_l} = \frac{(\mathrm{d_2} - \mathrm{d_1})}{(\mathrm{d_2} + \mathrm{d_1}) * \varepsilon * \mathrm{l_w} * \mathrm{d_p}} + \frac{4 * \mathrm{d_p} * \mathrm{l_{lhp}}}{\mathrm{d_l^4}} \qquad \mathrm{Geo_v} = \frac{\mathrm{d_p} * \mathrm{l_{lhp}}}{\mathrm{d_v^5}}$$

$$\mathrm{F_{ml*}} = \frac{\rho_l * \sigma * \lambda}{\mu_l} * \cos(\theta) \qquad \mathrm{F_{mv*}} = \rho_v * \lambda_{fg}^2 * \sigma * \cos(\theta)$$

Fluid Selection

Selection of working fluid is always directly connected with the respective thermo-physical properties of the fluid in its operating temperature range. Wallin [11], defined some important parameters to be considered in selecting the working fluid.

1. Compatibility with wick and wall materials.
2. Wettability of wick and wall materials.
3. Vapor pressure in the operating temperature range.
4. High latent heat.
5. High thermal conductivity.
6. Low liquid and vapor viscosities.
7. High surface tension.

Vapor pressure plays an important role in determining the maximum operating temperature of the fluid. Latent heat of vaporization transports much more heat than sensible heat, hence a high value of latent heat results in greater and efficient heat transfer. During the circulation of fluid, the flow resistance should be low and therefore the selected fluid should have a lower viscosity value. Vapor density decreases as the temperature decreases along the saturation curve, therefore at low temperatures the vapor velocity reaches the sonic velocity and thus choking the fluid flow. The temperature at which sonic limit is the lowest operating temperature of the fluid. A higher surface tension value indicates greater energy is required (in the form of heat) for the fluid molecule at the boundary to break free from the surface. If a fluid has low surface tension value then the returning fluid would be vaporized before reaching the evaporator and thus limiting the fluid circulation cycle.

Working fluids used in a heat pipe find their applications from 4 K [12] up to 1500 K [13]. Water works best in the temperature range 300-500 K, where its closest competitor is ammonia which works exceptionally well from 220-370 K. Ammonia and water performs well in their operating temperature range due to high latent heat of vaporization and surface tension. The uniqueness of water starts to fade after 450 K as the vapor pressure of water increases rapidly after it, whereas ammonia requires careful handling.

Chandratilleke et al. [12] demonstrated for the first time that a loop heat pipe can also function properly in cryogenic temperature. Heat pipes were demonstrated to work at 70 K, 28 K, 15 K and 4 K using different working fluids such as nitrogen, neon, hydrogen and helium respectively. Anderson et al [14] investigated different working fluid in the working temperature range of 450 K to 700 K. He observed that in the above temperature range several of the Halide salts, including titanium tetrachloride, tetra bromide and tetra iodide appears to be potential working fluids. Other potential fluids include aluminum, beryllium, bismuth, gallium, antimony, silicon and tin halides. Some of the organic fluids that work as expected in this temperature range are aniline, naphthalene, toluene, hydrazine, and phenol as long as they are not exposed to radiation.

Mercury find’s its temperature range of application from 600-900 K due to its supportive thermo-physical properties. Mercury was initially considered but later rejected as a working fluid liquid due to its wetting properties. Mercury does not properly wets the wick due to high contact angle. Although Deverall [13] reported successful functioning of mercury heat pipe when coarse magnesium was added to increase wetting. Apart from being a non-wetting liquid, mercury is also difficult to handle due to its toxicity.

In the temperature range 1200-2000 K [3] some liquid metals that find applications are cesium, potassium, sodium and lithium. Lithium with the highest merit number is the best in the group but lacks compatibility with almost all metal casing. At high temperatures lithium attacks almost every metal casing, it is therefore more convenient to use the next best in group i.e. sodium. Lithium at high temperature is compatible with only some elements in the periodic table and those are tungsten, tantalum, niobium and molybdenum. Use of such casing to resolve the compatibility issue is well documented by Wei [15].

For a fluid to return to the evaporator, a fluid with low liquid density and high surface tension is recommended. This phenomenon was studied by Asselman et al. [8]

and he formulated an important criterion for fluid selection. Asselman proposed that besides a high merit number, a high surface tension to liquid density ratio should also be considered for safe selection the fluid.

Fluid	ρ_l (kg/m^3)	σ (N/m)	σ/ρ_l (m^3/s^2)
Propene	608.4	$5.9*10^{-3}$	$9.7*10^{-6}$
Ammonia	681.4	$33.9*10^{-3}$	$49.8*10^{-6}$
Butane	604.0	$15.4*10^{-3}$	$25.5*10^{-6}$
Methanol	750.4	$18.8\text{-}10^{-3}$	$25.0*10^{-6}$
Ethanol	757.0	$17.3*10^{-3}$	$22.8*10^{-6}$
Water	958.8	$58.9*10^{-3}$	$61.5*10^{-6}$
Toluene	779.6	$18.0*10^{-3}$	$23.1*10^{-6}$

Table 3: Liquid Density to surface tension ration at normal boiling temperature [8]

Asselman was able to establish a trend in this ratio that can be easily used to predict the effectiveness of the working fluid. Water and ammonia (Table. 3), are exceptions in this group also, they are best used working fluids in their respective temperature range.

Thermo-physical Properties

Angirasa [16] listed the required thermodynamic properties for a potential heat pipe fluid in the intermediate temperature range (i.e. from 400 to 700 k). Other than Points 3 and 4 (of the under given points) all the requirements will also hold true for every other temperature range. The points listed were:

1. Wets a metallic solid surface (wick).
2. High latent heat of evaporation.
3. Melting point below ~400 K.
4. Critical point above ~800 K.

5. Chemically stable at high temperature.
6. Low liquid viscosity.
7. High surface tension.
8. Non-toxic.
9. Non-volatile.

In this part of the literature review we would specifically discuss the important properties of fluids and their methods of formulation as a function of temperature using only the intensive property and chemical structure. There are several ways of formulating such properties as a function of temperature, the best being is to obtain the data experimentally. Theoretically speaking, representing the property of the specified fluid as a polynomial function over the entire temperature range has been better utilized until now. But, there are some problems associated with such methods,

1. The polynomial coefficient varies with fluids.
2. They are calculated for only specified (mentioned) temperature range.
3. The polynomial function is usually curve fit, which increase the percentage error outside the temperature range.

For property formulation, we have tried to exclude the polynomial function completely. Instead, we have only used the pre-defined thermodynamic properties to formulate them as a function of operating temperature. This system of formulation is better than the previously used method in several ways. First, the thermodynamic properties are easily available and we do not have to worry about the polynomial functions. Second, it works well from the triple point to the critical point. Third, it does not requires a curve fitting procedure in order to specify points of relevance in any specific temperature range. The basic thermodynamic inputs for methods formulation are,

1. Intensive properties: Acentric factor, normal boiling and melting temperature.
2. Critical point parameters: Temperature, molar volume, pressure, compressibility factor.
3. Universal constants: Gas constant (R) and Stefan-Boltzmann constants (K).

Vapor Pressure and Latent Heat of Vaporization

The vapor pressure of the fluid in the operating temperature is an important parameter for fluid selection. High vapor pressure requires thick envelope walls as well as stronger welds to withstand the increasing pressure. The increased mass for stronger casing reduces the heat pipe performance. Low vapor pressure will result in a greater temperature gradient along the length of the heat pipe which makes it non-working at higher temperatures [16]. Anderson et al [14] observed that merit number for water was still increasing after the normal boiling point (which makes water a potential fluid to use), but the problem he noticed was that the vapor pressure had started to increase exponentially (see Fig. 7) just after the normal boiling temperature (from 1 atm @ 273 K to 25.16 atm @ 500 K), after which it was not considered safe to use water as a heat pipe fluid. Due to these limitations, alkali metals came into existence and were considered best after water from 450 K onwards.

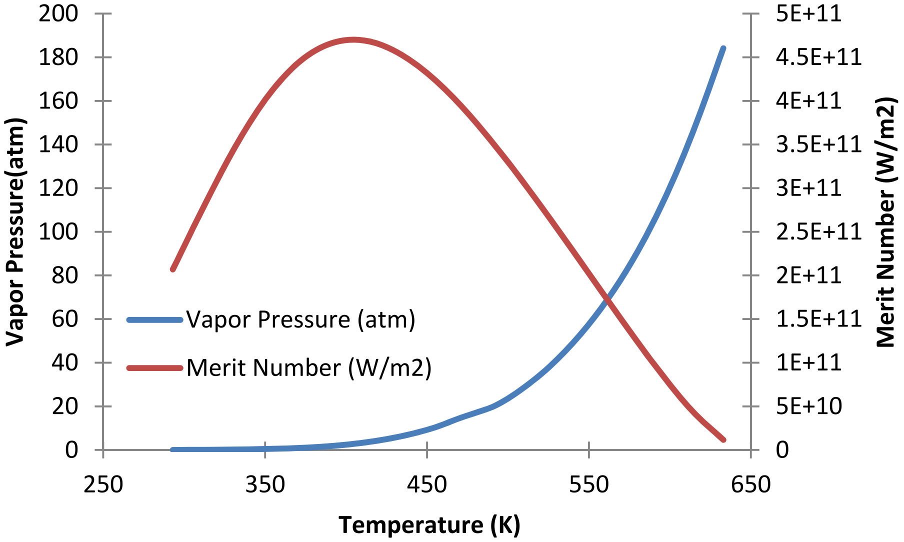

Figure 7: Merit number and vapor pressure curve for water.

Clausius-Clapeyron equation is a first order differential equation subjecting the dependence of saturation pressure and temperature for all fluids. When vapor and liquid exist in equilibrium close to the saturation curve, there exists an equality of chemical potential, temperature and pressure [17] which leads to the derivation of the Clausius-Clapeyron equation (Eq. 16). The two important characteristics of the equation are:

1. In (P) vs (1/T) graph always gives a negative slope.
2. The slope is always equal to.$-(\lambda/R)$

$$\frac{dP}{P} = \frac{\lambda}{R}\frac{dT}{T^2} \tag{16}$$

Vapor pressure for all fluids is calculated by integrating the above equation and assuming latent heat of vaporization to be constant (at the normal boiling point). Eq. 17 gives the Clausius-Clapeyron equation in its exact form ("A" being the integration constant).

$$ln(P_v) = A - \frac{(\lambda/R)}{T} \tag{17}$$

Antoine [18] (Eq. 18) corrected the Clausius-Clapeyron equation by introducing a constant to the temperature term. Antoine believed that Clausius-Clapeyron equation cannot be accurately applied over on the larger range of temperature (specifically for T_R over 0.75 and for the fluids with low boiling point). Adding the constant make the equation suitable for a larger temperature range.

$$ln(P_v) = A - \frac{(\lambda/R)}{T + C} \tag{18}$$

Wagner [19] used the statistical method combined with Clausius-Clapeyron equation to develop an empirical formula for vapor pressure of argon and nitrogen on the entire temperature range (whose experimental values were known). It was later established as an equation (Eq. 19), which can be used for all fluids and was found accurate even over $T_r \geq 0.7$. The constants in Eq.19 were calculated by Forero et al. [20], who developed a method to calculate the constant for more than 274 pure substances with high accuracy. The vapor pressure from 0.01 atm to critical pressure was calculated with an average deviation of 0.039% only. Forero et al. even established a generalized relation of all the constants (Francis Constants A, B C and D in the Eq. 19) making then a function of acentric factor only.

$$\ln\left(\frac{\mathrm{P}}{\mathrm{P_c}}\right) = \frac{\mathrm{Ar} + \mathrm{Br}^{1.5} + \mathrm{Cr}^{2.5} + \mathrm{Dr}^{5}}{1 - \mathrm{r}} \tag{19}$$

$$\text{where } \mathrm{r} = 1 - \frac{\mathrm{T}}{\mathrm{T_c}}$$

These equations work well in estimating the vapor pressure over the entire range of temperature except near the critical temperature, where λ is a weak function of temperature and vapor pressure is is tend to achieve abnormally high values. Hence it become clear that in order to increase the accuracy of the vapor pressure at higher temperatures, mainly $T_r > 0.7$, a three parameter equation must be preferred over Clausius-Clapeyron two parameter state equations. Pitzer [21] in 1955 suggested that a third parameter is required for defining all the thermodynamic states of the fluid and gasses. Since the intermolecular forces in complex molecules is a sum of interaction between various part of the molecule and is not concentrated around the central part of the molecule, hence a new concept of acentric factor was suggested. Acentric factor (Eq. 20) was defined by Pitzer as the measure of the deviation in the properties over reduced temperature of 0.7. Acentric factor is a temperature independent property, whose values differ for different fluids. The reduced pressure P_r is calculated at $T_r = 0.7$. Pitzer three parameter equation (Eq. 21) was suggested after realizing the fact that vapor pressure can also a function of reduced temperature. The values of z_o and z_1 for different fluids are tabulated in his paper over the entire range of reduced temperature.

$$\omega = -\log(P_r) - 1.0 \qquad (20)$$

$$\ln P = z_o(T_r) + \omega * z_1(T_r) \qquad (21)$$

Lee et al. [22] (Eq. 21) described a method of representing a thermodynamic function based on Pitzer's three parameter state. This analytical form tends to increase the reliability of values near the critical temperature. The idea which lead them to realize that highly accurate vapor pressure can be now formulated was inspired by the fact that the compressibility factor constants (z_0 and z_1) were also the function of reduced temperature (Eq. 22 a & b)

$$z_o = 5.92714 - \frac{6.09648}{T_r} - 1.28862 * \ln(T_r) + 0.169347 \ * T_r^6 \tag{22 a}$$

$$z_1 = 15.2518 - \frac{15.6875}{T_r} - 13.4721 * \ln(T_r) + 0.43577 \ * T_r^6 \tag{22 b }$$

Latent heat of vaporization gradually decreases with increase in temperature and vanishes at the critical temperature. Watson [23] (Eq. 23) expressed the dependence of latent heat of vaporization on reduced temperature through the following empirical formula. Subscript "k" is the reference latent heat of vaporization at a known temperature.

$$\lambda = \lambda_k \left(\frac{1 - T_r}{1 - T_{r_k}}\right)^n \tag{23}$$

The indices "n" was decided as 0.38 by Watson, but Viswanath et al. [24] (Eq. 24) recommended that this parameter not to be a constant but differs for different fluids (although very close to 0.38 for all fluids).

$$n = \left(0.00264 \left(\frac{\lambda_b}{R\,T_b}\right) + 0.8794\right)^{10} \tag{24}$$

Watson's equation requires the latent heat of vaporization at a known temperature, for which latent heat of vaporization at the normal boiling point was considered as a potential solution. Riedel [25] (Eq. 25 a) proposed one of the first equations for latent heat at normal boiling temperature. His equation used only critical parameters and R (universal gas constant). Chen [26] (Eq. 25 b) and Viswanath et al. [24] (Eq. 25 c) gave the same kind of empirical formula. Chen and Viswanath et al. did not used any other constants (like "R") to better fit the values.

$$\lambda_b = 1.093\,R\,T_b\left(\frac{\ln(P_c) - 1.013}{0.93 - T_{r_b}}\right) \tag{25 a}$$

$$\lambda_b = T_b\left(\frac{(7.11\log_{10} P_c) - (7.9\,T_{r_b}) - 7.82}{1.07 - T_{r_b}}\right) \tag{25 b}$$

$$\lambda_b = 4.7\ T_c \log(P_{r_b})\left(\frac{(1 - P_{r_b})^{0.69}}{1 - \frac{1}{T_{r_b}}}\right) \tag{25 c}$$

Pitzer [27] also established a formula in which latent heat of vaporization is a function of critical temperature and acentric factor. The analytical representation of the latent heat as a function of temperature is given below (Eq. 26). This equation was found to work very accurately in the range $0.5 \le T_r \le 1.0$.

$$\frac{\lambda}{R\,T_c} = 7.08\,(1 - T_r)^{0.354} + 10.95\,\omega\,(1 - T_r)^{0.456} \tag{26}$$

Density

Density of the fluid is a property which finds its presence directly or indirectly in every thermo-dynamical system and in wide variety of engineering calculations. An extensive literature is available by different researchers determining the densities of various compounds (in their pure state or in mixtures). The calculative form of density (vapor density) founded its application back in 1873 in the form of Van der Waals equation (Eq. 27) of state for gasses.

$$\rho = \frac{P * M}{R * T} \tag{27}$$

A. Liquid Density

Liquid density varies inversely as a function of temperature which can be written in the form of Eq. 28. The critical point was again the problem and the percentage deviation of the property values near the critical point were extremely high. Francis [28]

$$\rho = \mathrm{A} + \left(\frac{\mathrm{B}}{\mathrm{T}}\right) \tag{28}$$

stated that saturated liquid densities can be expressed as a quadratic function (as initially it was treated linear, see Eq. 28) over the entire range of temperature. His equation (Eq. 29) tries to correct the liquid density as close as possible to the critical point. Introducing a linear temperature variation term to the equation improved the accuracy at higher temperatures. The constants in Eq. 29 were uniquely chosen "A" is slightly higher than the liquid density at low temperature (close to normal-melting point),

$$\rho_s = \mathrm{A} - \mathrm{Bt} - \frac{\mathrm{C}}{\mathrm{E} - \mathrm{t}} \tag{29}$$

"B" is slightly less than the temperature coefficient of liquid density, "C" is a small integer depending upon the slope of the isochor $(dP/dt)_V$ and E is usually slightly larger than the critical temperature [28]. These constants for approximately 130 pure compounds are listed in his work.

Yen et al. [29] gave a generalized equation (Eq. 30) relating reduced density to reduced temperature. Being a continuation to Francis works Eq. 30 reduces the average percentage deviation and near the critical temperature by introducing the compressibility factor at the critical point for the first time. Yen et al. believed that increasing the polynomial index of the equation would give good results at lower temperatures. The constants in the equation were applied to sixty-two pure compounds whose critical compressibility factor ranged from 0.21 to 0.29, the calculated value had a maximum deviation of only 2.1 % [29].

$$\rho_{rs} = \frac{\rho_s}{\rho_c} = 1 + A(1 - T_r)^{\frac{1}{3}} + B\,(1 - T_r)^{\frac{2}{3}} + D(1 - T_r)^{\frac{4}{3}} \tag{30}$$

$$A = 17.4425 - 214.578 * Z_c + 989.625 * Z_c^2 - 1522.06\, Z_c^3 \tag{30 a}$$

$$B = -3.28257 + 13.6377\, Z_c + 107.4844\, Z_c^2 - 384.211\, Z_c^3 \qquad \text{if } Z_c \leq 0.26 \tag{30 b}$$

$$B = 60.2091 - 402.063\, Z_c + 501\, Z_c^2 + 641.0\, Z_c^3 \qquad \text{if } Z_c > 0.26 \tag{30 c}$$

$$D = 0.93 - B \tag{30 d}$$

Riedel [30] in 1954 changed the form of the equation from two parameter state equation to three parameter state equation by introducing acentric factor to his equations (Eq. 31). His endeavors were initially focused on the molar volume (cm^3/mole) but finally an equation for liquid density was formulated (see Eq. 31).

$$\rho_{rs} = \frac{\rho_s}{\rho_c} = \frac{V_c}{V_s} = 1 + (1.69 + 0.984\omega)(1 - T_r)^{\frac{1}{3}} + 0.85(1 - T_r) \tag{31}$$

Pitzer et al in 1965 gave an empirical formula for showing the dependence of the liquid molar density on temperature in terms of critical parameters. Lyckman et al. [27] in 1964 showed that due to the linear nature of the Pitzer equation, the calculated molar densities were deviating the literature data therefore he modified the Pitzer equation and presented a corrected equation (Eq. 32) which was a quadratic equation in acentric factor. The generalized parameters are a function of the reduced temperature and are

$$\frac{V}{V_c} = V_r^0 + \omega V_r^1 + \omega^2 V_r^2 \tag{32}$$

experimentally calculated by the studying density data of argon, nitrogen, ethylene, propane, carbon tetrachloride, benzene and heptane. Appendix “A” describes the nature of the generalized functions. The generalized function V_r^0 increases with increasing temperature and returns a unity value at the critical parameter. The other generalized function also follows a similar pattern. An equation for the critical molar volume was also given by Lyckman et al. (Eq. 33).

$$\mathrm{V_c} = \left(\mathrm{R} * \frac{\mathrm{T_c}}{\mathrm{P_c}}\right)(0.291 - 0.08\omega) \tag{33}$$

Gunn et al. [31], replaced critical molar volume from scaling molar volume. His equation (Eq. 34) was valid over the entire range of the temperature i.e. $0.2 \leq T_r \leq 1.00$. The equation was linear in acentric factor.

$$\frac{\mathrm{V}}{\mathrm{V_{SC}}} = \mathrm{V_R^0}(1.0 - \omega * \delta) \tag{34}$$

The generalized parameter $\mathrm{V_R^0}$ and δ are a function of reduced temperature only, which were calculated from the density data available for the following 10 substances: argon, methane, nitrogen, propane, n-pentane, n-heptane, n-octane, benzene, ethyl-ether and ethyl-benzene [31]. Gunn et al used scaling volume instead of the critical volume which increased its accuracy near the critical point. The generalized function $V_{0.6}$ (Eq. 35) is the molar volume of the fluid at reduced temperature of 0.6. The value of V_{SC} for some compounds can be found in Appendix B, for other the formula (Eq. 35) works fine.

$$\mathrm{V_{SC}} = \frac{\mathrm{V_{0.6}}}{0.3862 - 0.0866\omega} \tag{35}$$

B. Vapor Density

The first successful attempt of modifying and correcting the ideal gas equation to be applicable for real gasses was done by Van Der Waals in 1873 [32]. Some changes were proposed in the specific volume and pressure terms (Eq. 36) after studying the behavioral pattern of intermolecular forces at high pressures. The constants “a” and “b” used in Eq. 36 are obtained by evaluating the isothermal properties of fluid at the point of inflection or at the critical point (Eq. 37).

$$\left(\mathrm{P}+\frac{\mathrm{a}}{\mathrm{v}^2}\right)(\mathrm{v}-\mathrm{b})=\mathrm{RT} \tag{36}$$

$$\left(\frac{\partial \mathrm{P}}{\partial \mathrm{v}}\right)_{\mathrm{T_c}}=0 \qquad \left(\frac{\partial^2 \mathrm{P}}{\partial^2 \mathrm{v}}\right)_{\mathrm{T_c}}=0 \tag{37}$$

Redlich-Kwong (1949) introduced some corrections in the van der waals equation which can be seen in Table. 4. Stepping up from two parameter corresponding state equation to three parameter corresponding state equation, Soave (1972) and Peng-Robinson (1976) introduced the acentric factor to the parameter “b”. All these equations are individually known as the cubic equation of state (Eq. 38), since the equation is cubic in molar volume. The constants can be calculated from the Table. 4.

$$\mathrm{P}=\frac{\mathrm{RT}}{\mathrm{v}-\mathrm{b}}-\frac{\mathrm{a}}{\mathrm{v}^2+\mathrm{ubv}+\mathrm{wb}^2} \tag{38}$$

Equation	u	w	a	b
Van Der Waals	0	0	$\frac{RT_c}{8P_c}$	$\frac{27}{64}(\frac{R^2T_c^2}{P_c})$
Redlich-Kwong	1	0	$\frac{0.08664RT_c}{P_c}$	$0.42748(\frac{R^2T^{2.5}}{P_c\ T^{\frac{1}{2}}})$
Soave	1	0	$\frac{0.08664RT_c}{P_c}$	$0.42748\left(\frac{R^2T_c^2}{P_c}\right)\left[1+f\omega\left(1-T_r^{\frac{1}{2}}\right)\right]^2$ $where\ f\omega = 0.48 + 1.574\omega - 0.176\omega^2$
Peng-Robinson	2	-1	$\frac{0.07780RT_c}{P_c}$	$0.45724\left(\frac{R^2T_c^2}{P_c}\right)\left[1+f\omega\left(1-T_r^{\frac{1}{2}}\right)\right]^2$ $where\ f\omega = 0.37464 + 1.54226\omega - 0.26992\omega^2$

Table 4: Constants for cubic equation of state [33]

Surface Tension

Surface Tension is defined as the force exerted on the phase boundary per unit length, making it an extremely relevant property associated with fluid selection. The surface tension of the fluid varies linearly with the temperature i.e. with the increase in temperature, the surface tension of the fluid decreases linearly and vanishes at the critical temperature. Fig. 8 shows the variation of surface tension with temperature of various fluids. In the reduced temperature range 0.45 to 0.65, the surface tension for most of the organic fluids range from 0.02 to 0.04 N/m [33]. The surface tension of water at 293 K is 0.0728 N/m [34] and for various liquid metals it ranges from 0.3 to 0.6 N/m [34].

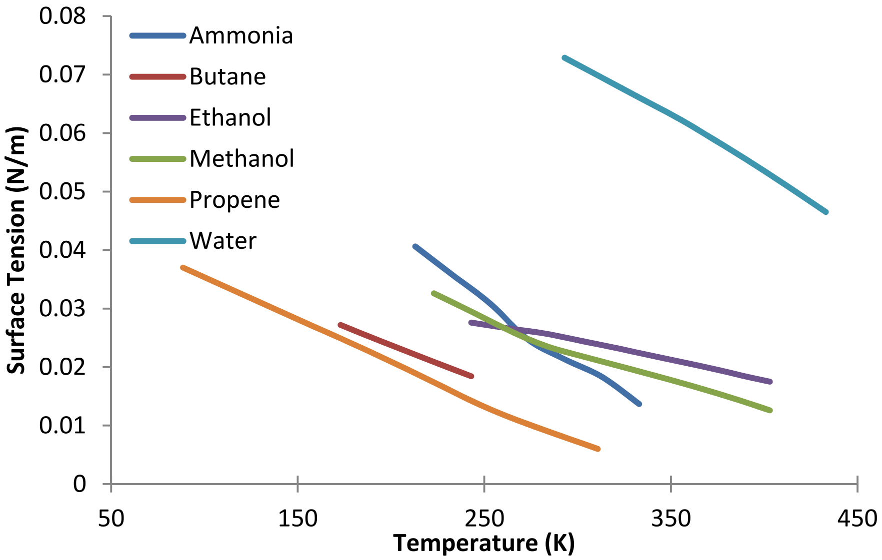

Figure 8: Surface Tension of various fluids [3, 35]

High surface tension of water makes it one of the most useful fluid in the given operating range. More relevant properties are often unavailable for less common fluids. Surface tension, according to Dunbar and Cadell [10] is the least documented property. Some correlations exist between documented properties and the surface tension but most of these are based on the concept given by the Macleod correlation [36]. Macleod suggested that thermo-physical properties such as surface tension, latent heat and critical temperature of the liquid are closely connected with the cohesive forces in the van der Waals equation (being largely dependent on the internal forces between molecules). With the increase in temperature, the intermolecular distance increases, van der waals equation show that the intermolecular forces falls with the 4th power of the intermolecular distances. Therefore, it can be assumed that surface tension is the function of the intermolecular distances and is closely connected to the density of the fluid.

The Empirical formula given by Macleod [36] in 1923 suggested a linkage between surface tension and respective state densities (liquid and gaseous) which can be seen in Eq. 39. “C” fits the experimental data for all fluids with good accuracy from melting point to approximately 40 K below the critical temperature. Macleod further observed that C is a temperature independent property over the entire operating range.

$$\frac{\sigma^{\frac{1}{4}}}{(\rho_l - \rho_v)} = C \tag{39}$$

Samuel Sudgen [37], after carefully studying the behavioral pattern of the Macleod’s correlation gave two empirical relations which involve surface tension and the critical parameters as a function of temperature (see Eq. 40a and Eq. 40b). “K_1” and “K_2” are

$$\sigma = K_1 T_c \left(Vc^{-\frac{2}{3}}\right) * (1 - T_r)^{1.2} \tag{40 a}$$

$$\sigma = K_2 T_c^{\frac{1}{3}} \left(Pc^{\frac{2}{3}}\right) * (1 - T_r)^{1.2} \tag{40 b}$$

constants. Sudgen even worked on the temperature independent parameter of Macleod and indicated how it may be calculated from the structure of the fluid. He also acknowledged Macleod findings with relevance to experimental data and summarized that Macleod’s relation between surface tension and density is found to be true from the melting point to 40 K below the critical temperature. He called this constant as Parachor and changed the liquid and vapor density to respective molar liquid and vapor density. The Sudgen atomic and structural Parachor value can be found in appendix C.

Vargaftik et al. [34] in 1983 working on the surface tension of water established experimental surface tension relation of water as a function of temperature from melting temperature to the critical temperature (T_r = 0.9). Verifying the work of Sudgen [18] with the critical temperature of water as 647.15 K, he interpolated the equation of surface tension (Eq. 41) as a function of temperature in the pattern suggested by Sudgen.

$$\sigma = \left(235.8 * 10^{-3} * \left(1 - 0.625(1 - T_r)\right)\right) * (1 - T_r)^{1.2} \tag{41}$$

Quale [38] studied the experimental surface tension value and density data for various compounds and calculated his structural Parachor. He then suggested the additive pattern for calculating the Parachor. The Quale structural Parachor can be found in appendix D.

Brock et al. [39] in 1955 related all the work that has been done on surface tension and suggested that surface tension can also be accurately estimated using an empirical equation relating critical properties and normal boiling points. This method was helpful in estimating surface tension again as a function of temperature without having the knowledge of the structure of the compound. Brock's equation (Eq. 42) is an extended work of Sudgen's correlation (Eq. 40 b)

$$\sigma = P_c^{\frac{2}{3}}\, T_c^{\frac{1}{3}}\, Q\, (1 - T_r)^{\frac{11}{9}} \tag{42 a}$$

where $$Q = 0.1196\left(1 + \frac{T_{br} \ln\left(\frac{P_c}{1.01325}\right)}{(1 - T_{br})}\right) - 0$$

Viscosity

Viscosity, also known as the internal friction of fluid, is defined as the shear stress over the velocity gradient. It tends to oppose any change in the dynamics of the fluid movement by acting as an opposing force between fluid layers. A low viscosity between fluid layers signifies higher velocity gradient which in turn results in less opposed fluid flow. Viscosity is not the equilibrium property as density is, which when grouped with different thermodynamic data is useful for developing co-relations between complex fluid flows.

A. Liquid Viscosity

Liquid viscosity is higher than the vapor viscosity at the same saturation temperature. For example, the liquid viscosity of water at the normal boiling point is approximately 23 times higher than the vapor viscosity, which is about 34 times for ammonia. For a temperature range from the melting point to the normal boiling point and further to the critical temperature, it is often a good approximation to assume that $\ln(\mu_l)$ is inversely proportional to temperature The simplest explanation for this approximation was first mentioned by Guzman in 1913 (Eq. 43). Vogel equation (Eq. 44) was only an improvement of previous equation by adding a constant term to temperature.

$$\ln(\mu_l) = A + \frac{B}{T} \tag{43}$$

$$\ln(\mu_l) = A + \frac{B}{T + C} \tag{44}$$

If the value of liquid viscosity at a temperature is known, then Lewis-Squire chart can be used to extrapolate the viscosity over the entire temperature range, or simply by using Eq. 45. Given a known value at any temperature, liquid viscosity can be easily formulated over the entire temperature range.

$$(\mu_l)^{-0.2661} = (\mu_l)_k^{-0.2661} + \frac{T - T_k}{233} \tag{45}$$

Reid and Polling [33] have used the three equations given below (Eq. 46 a - c) to formulate viscosity as a function of temperature for almost all know fluids, for which constants can also be found in their work.

$$\mu_l = AT^B \tag{46 a}$$

$$\ln(\mu_l) = A + \frac{B}{T} \tag{46 b}$$

$$\ln(\mu_l) = A + \frac{B}{T} + CT + DT^2 \tag{46 c}$$

B. Vapor Viscosity

Molecular Collisions of gaseous particle cause a change of momentum. Chapman-Enskog [10] after studying this transport property of momentum at the molecular level developed a vapor viscosity relation (Eq. 47) for a rigid, non-interacting sphere model. The Collision integral was assumed to be 1 for the nonpolar molecules and slightly

$$\mu_v = 26.69 * \frac{(M * T)^{\frac{1}{2}}}{d_{\text{sphere}}^2 \ni_v} \tag{47}$$

higher than 1 for polar molecules. Chapman-Enskog proposed the empirical relation but spherical diameter and the collision integral were still a point of concern. The collision integral has been now determined by a number of researchers, but the most used method was given by Neufeld et al. [40]. He defined a dimensionless temperature relating to the potential energy stored in the molecular (Eq. 48). The collision integral relation, which according to Neufeld has an average deviation of only 0.64% is given in Eq. 49.

$$\mathrm{T}_{*} = \frac{\mathrm{k} * \mathrm{T}}{\gamma} \tag{48}$$

$$\ni_{\mathrm{v}} = [1.1614(\mathrm{T}_{*})^{-0.14874}] + 0.524[\exp(-0.7732\mathrm{T}_{*})] + 2.161[\exp(-2.43787\mathrm{T}_{*})] \tag{49}$$

Chung et al. [41] simplified the Neufeld dimensionless temperature and it was written as only the function of critical temperature. The spherical diameter was also simplified as a function of critical molar volume. Introduction of dipole moment into the equation separates Chung equation (Eq. 50) from all other works which was in turn responsible for shaping the value of collision integral. This equation also works fine for nonpolar fluids. Finally, the Chung equation is a three parameter corresponding state equation which directly depends upon the critical parameters, acentric factor and dipole moment of the fluid for formulating vapor viscosity as a function of temperature.

$$\mu = 40.785 * \frac{\left(\mathrm{F}_{\mathrm{c}}\,(\mathrm{MT})^{\frac{1}{2}}\right)}{\mathrm{V}_{\mathrm{c}}^{\frac{2}{3}} * \ni_{\mathrm{v}}} \tag{50}$$

$$\mathrm{F}_{\mathrm{c}} = 1 - 0.2756 * \omega + 0.059035 * \mu_{\mathrm{r}}^{4} \tag{50 a}$$

$$\mu_{\mathrm{r}} = 131.3 * \frac{\mathrm{p}_{\mathrm{c}}}{(\mathrm{V}_{\mathrm{C}} * \mathrm{T}_{\mathrm{c}})^{\frac{1}{2}}} \tag{50 b}$$

Lucas [33] realized the importance of dimensionless inverse reduced viscosity and finally linked it to the reduced temperature. His equation was further simplified by Thodos et al. [42] (Eq. 51) and worked accurately until Tr = 0.9. The difference was the use of a compressibility factor at the critical point, hence making it a two parameter corresponding state equation.

$$\mu\,\epsilon = (0.606\ \mathrm{T_r})\mathrm{F_p^0} \tag{51}$$

$$\epsilon = 0.176\left(\frac{\mathrm{T_c}}{\mathrm{M^3\ P_c^4}}\right)^{\frac{1}{6}} \tag{51 a}$$

$$\mathrm{F_p^0} = 1 + 30.55(0.292 - \mathrm{Z_c})^{1.72}\ ;\ \ 0.022 \le \left(52.46 * \frac{\mathrm{p^2\ P_c}}{\mathrm{T_c^2}}\right)\ \ ;\ \ \mathrm{F_p^0} = 1 \tag{51 b}$$

CHAPTER 3

RESULTS AND DISCUSSION

Thermal Fluids and Working Temperature Range

In this work, we have classified thermal fluids as Polar and Nonpolar fluids. The polar fluids were sub classified as organic and Inorganic fluids. The fluids of interest are water, ammonia, methanol and ethane. The entire temperature range was covered from cryogenic (ammonia) to intermediate temperature of 450-500 K (water).

1. Polar Fluids
    a. Inorganic fluids: Water and Ammonia.
    b. Organic Fluids: Methanol
2. Nonpolar Fluids: Ethane

The important thermodynamic properties of all these four fluids were calculated using the methods briefly described in chapter 2. Error graphs (discussed later in this chapter) were plotted with reference to the experimental data available in [43]. Every method of property formulation was evaluated on the basis of the following parameters:

1. Input requirements
2. Works good with which type of fluid.
3. Operational temperature range.
4. Expected error percentage.

The critical parameters, as the input parameters for every fluids are critical temperature, pressure, molar volume and compressibility factor, which are taken for [33, 35]. Other input parameters include the molecular weight, acentric factor, normal freezing point, normal boiling point, dipole moment, some structural parameters like generalized reduced temperature parameter (Appendix A) , scaling molar volume (Appendix B), Sudgen structural Parachor (Appendix C) and Quale structural Parachor (Appendix D).

The rule of thumb for the maximum operating temperature of a fluid is about 100 K below its critical temperature [16]. Considering that the vapor pressure of the fluid should not exceed 25 atm, we have tried to select the operating temperature as close as possible to the critical temperature. Hence, for a higher range of working temperatures, the upper limit of the operating temperature range is set depending on which of the two given below states is achieved first.

- The maximum operating temperature for a fluid is about 40 K below the critical temperature.
- The vapor pressure should not exceed 25-30 atm.

Vapor density at lower saturation temperatures is extremely low, which results in very high vapor velocities, sometimes reaching sonic velocity. This is an important parameter of concern in deciding the lower limit of the operational temperature range.

Working Temperature (Kelvin)	Polar Fluids			Nonpolar
	Inorganic		Organic	Organic
	Ammonia	Water	Methanol	Ethane
	230-340	350-480	330-470	170-270

Table 5: Operating Temperature range for fluids

Latent Heat of Vaporization

Pitzer Equation

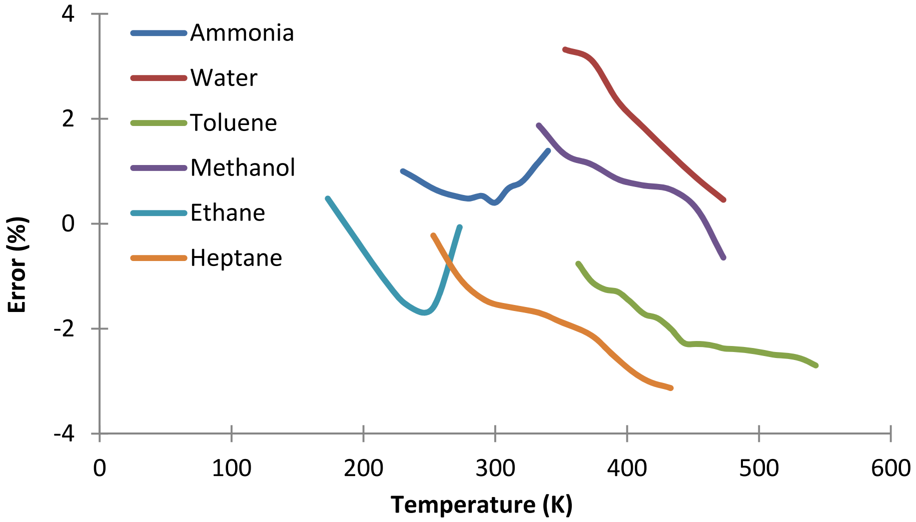

Figure 9: Pitzer equation error

Inputs Required

- Critical Parameters :Temperature
- Acentric Factor
- Universal Gas Constant (R)

Types of compound		Temperature range (Reduced temperature T_r)	Expected error (average)
Polar	Organic	$0.3 \leq T_r \leq 0.9$	$0 \leq \% \leq 3$
	Inorganic	$0.3 \leq T_r \leq 0.9$	$0 \leq \% \leq 4$
Nonpolar		$0.3 \leq T_r \leq 0.9$	$0 \leq \% \leq 3$

Table 6: Pitzer equation parameter table

Watson-Riedel Equation

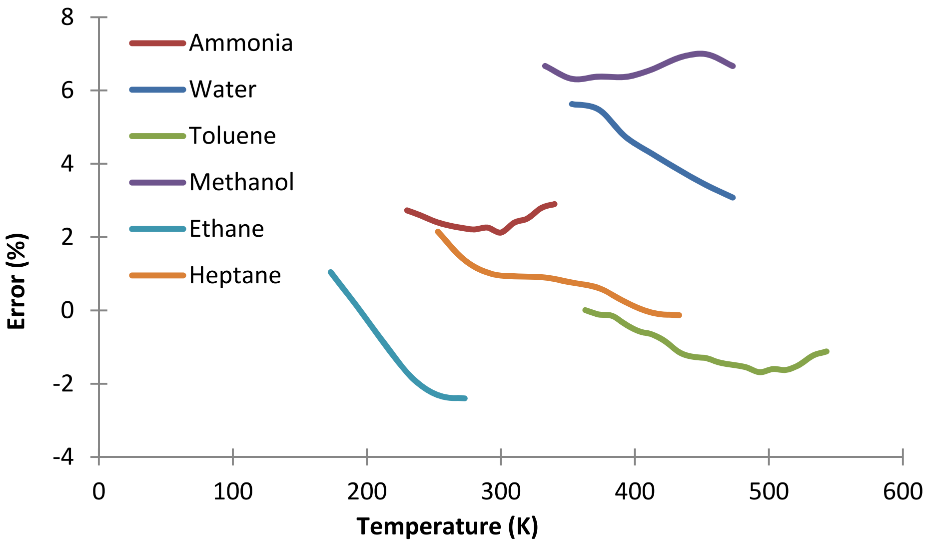

Figure 10: Watson-Riedel equation error

Inputs Required

- Critical Parameters: Temperature, Pressure
- Boiling Temperature
- Universal Gas Constant (R)

Types of compound		Temperature range (Reduced temperature T_r)	Expected error (average)
Polar	Organic	$0.3 \le T_r \le 0.9$	$0 \le \% \le 8$
	Inorganic	$0.3 \le T_r \le 0.9$	$0 \le \% \le 6$
Nonpolar		$0.3 \le T_r \le 0.9$	$0 \le \% \le 2$

Table 7: Watson-Riedel equation parameter table

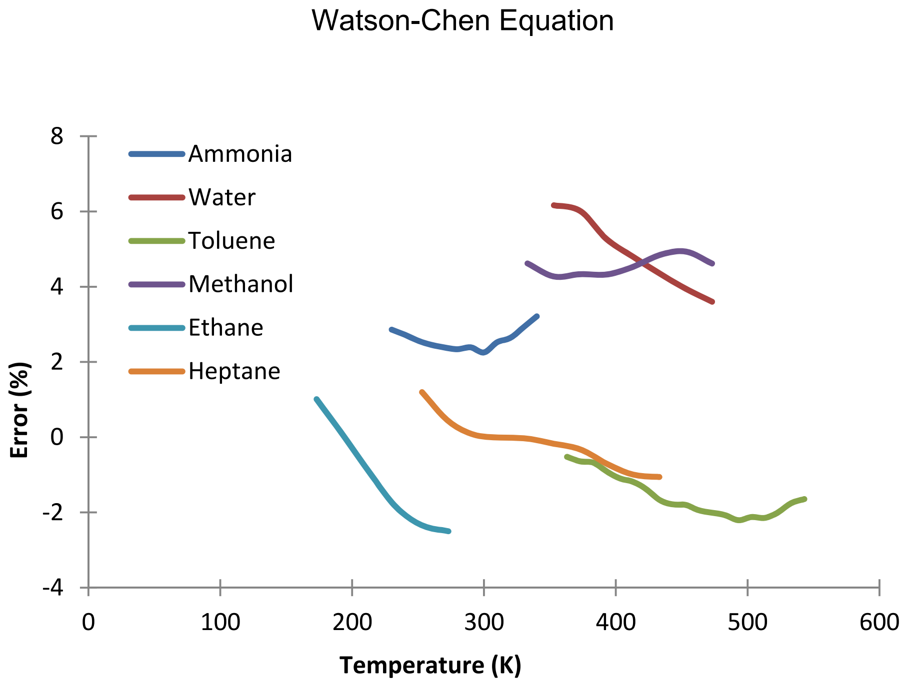

Figure 11: Watson-Chen equation error

Inputs Required

- Critical Parameters: Temperature, Pressure
- Normal boiling temperature
- Latent heat of vaporization at normal boiling temperature.

Types of compound		Temperature range (Reduced temperature T_r)	Expected error (average)
Polar	Organic	$0.3 \le T_r \le 0.9$	$0 \le \% \le 5$
	Inorganic	$0.3 \le T_r \le 0.9$	$0 \le \% \le 7$
Nonpolar		$0.3 \le T_r \le 0.9$	$0 \le \% \le 3$

Table 8: Watson-Chen equation parameter table

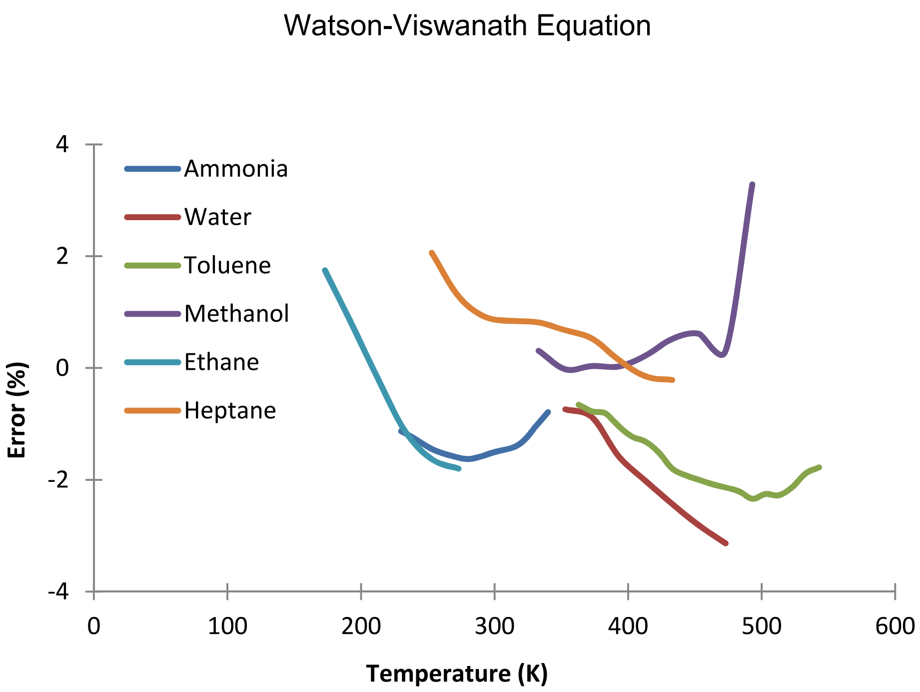

Figure 12: Watson-Viswanath equation error

Inputs Required

- Critical Parameters: Temperature, Pressure
- Boiling Temperature at all saturation pressure.
- Latent heat of vaporization at normal boiling temperature.

Types of compound		Temperature range (Reduced Temperature T_r)	Expected error (average)
Polar	Organic	$0.3 \leq T_r \leq 0.9$	$0 \leq \% \leq 5$
	Inorganic	$0.3 \leq T_r \leq 0.9$	$0 \leq \% \leq 4$
Nonpolar		$0.3 \leq T_r \leq 0.9$	$0 \leq \% \leq 3$

Table 9: Watson-Viswanath equation parameter table

Liquid Density

Francis et al. Equation

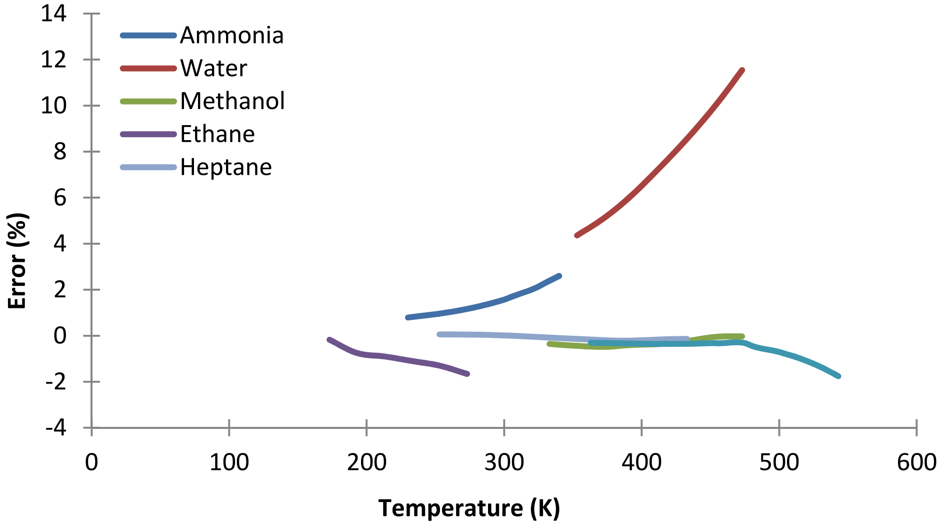

Figure 13: Francis et al. equation error

Inputs Required

- Francis Constants T_r
- Critical Parameters: temperature

Types of compound		Temperature range (Reduced Temperature T_r)	Expected error (average)
Polar	Organic	$0.2 \leq T_r \leq 0.9$	$0 \leq \% \leq 1$
	Inorganic	$0.2 \leq T_r \leq 0.9$	$0 \leq \% \leq 12$
Nonpolar		$0.2 \leq T_r \leq 0.9$	$0 \leq \% \leq 1$

Table 10: Francis et al. equation parameter table

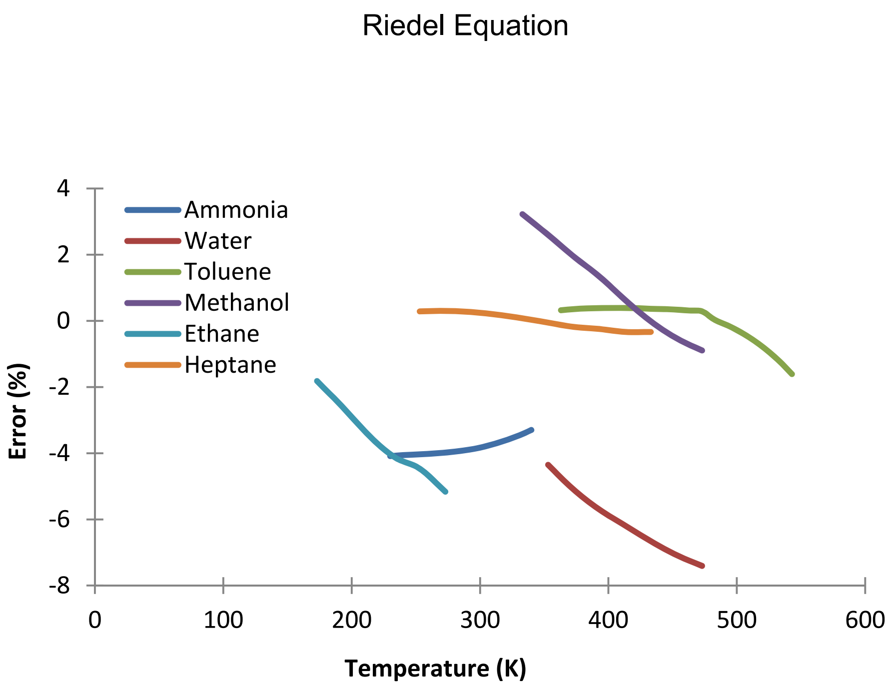

Figure 14: Riedel equation error

Inputs Required

- Acentric Factor
- Critical Parameters: Volume and Temperature

Types of compound		Temperature range (Reduced Temperature T_r)	Expected error (average)
Polar	Organic	$0.3 \leq T_r \leq 0.9$	$0 \leq \% \leq 4$
	Inorganic	$0.3 \leq T_r \leq 0.9$	$0 \leq \% \leq 7$
Nonpolar		$0.3 \leq T_r \leq 0.9$	$0 \leq \% \leq 5$

Table 11: Riedel equation Parameter table

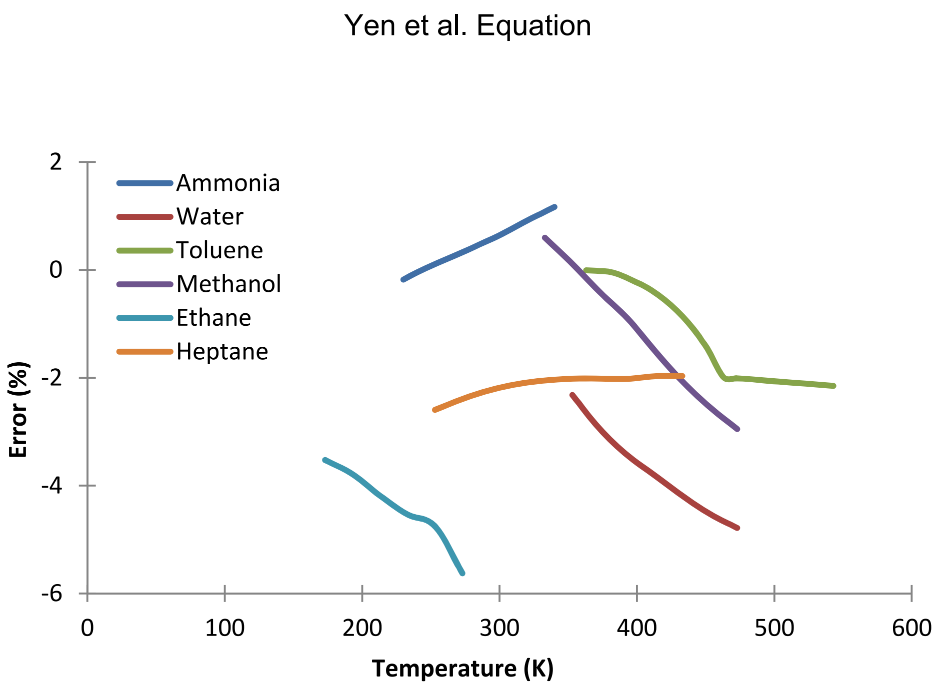

Figure 15: Yen et al. equation error

Inputs Required

- Critical Parameters: Compressibility factor, Temperature

Types of compound		Temperature range (Reduced Temperature T_r)	Expected error (average)
Polar	Organic	$0.3 \le T_r \le 0.9$	$0 \le \% \le 4$
	Inorganic	$0.3 \le T_r \le 0.9$	$0 \le \% \le 3$
Nonpolar		$0.3 \le T_r \le 0.9$	$0 \le \% \le 6$

Table 12: Yen et al. equation parameter table

Gunn et al. Equation

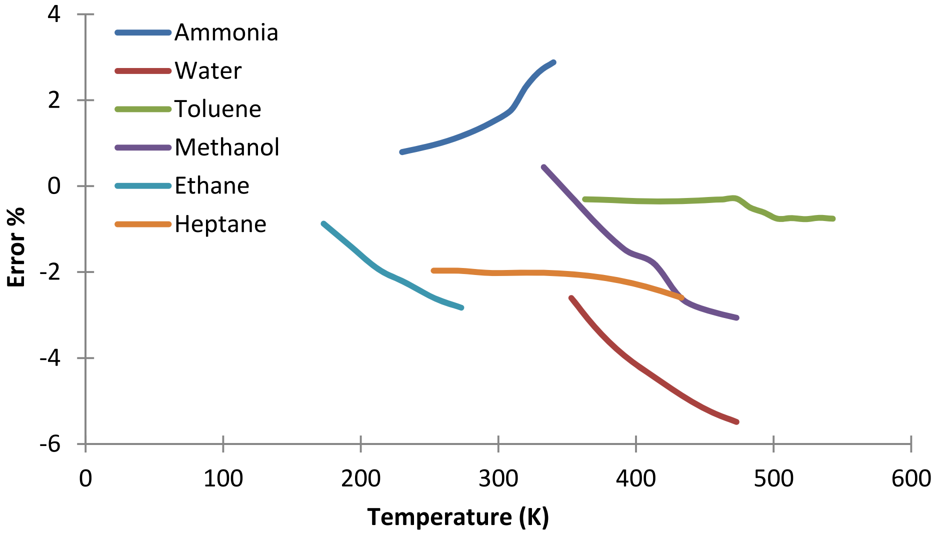

Figure 16: Gunn et al. equation error

Inputs Required

- Acentric factor
- Critical Parameters: Temperature
- Scaling velocity (Molar volume at $\square_{\square} = 0.6$)

Types of compound		Temperature range (Reduced Temperature T_r)	Expected error (average)
Polar	Organic	$0.2 \le T_r \le 0.9$	$0 \le \% \le 3$
	Inorganic	$0.2 \le T_r \le 0.9$	$0 \le \% \le 6$
Nonpolar		$0.2 \le T_r \le 0.9$	$0 \le \% \le 3$

Table 13: Parameter Gunn et al. equation parameter table

Vapor Density

Van der Waals Equation

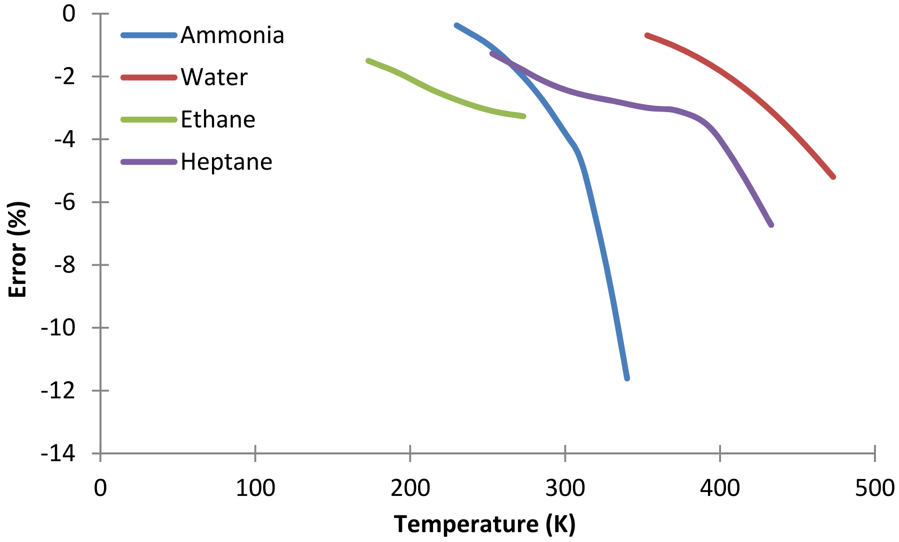

Figure 17: Van-der Waal’s equation error

Inputs Required

- Critical Parameters: Pressure, Temperature, Volume

Types of compound		Temperature range (Reduced Temperature T_r)	Expected error (average)
Polar	Organic	$0.4 \leq T_r \leq 0.9$	$\% \leq 30$
	Inorganic	$0.4 \leq T_r \leq 0.9$	$0 \leq \% \leq 10$
Nonpolar		$0.4 \leq T_r \leq 0.9$	$0 \leq \% \leq 5$

Table 14: Van-der Waal’s equation parameter table

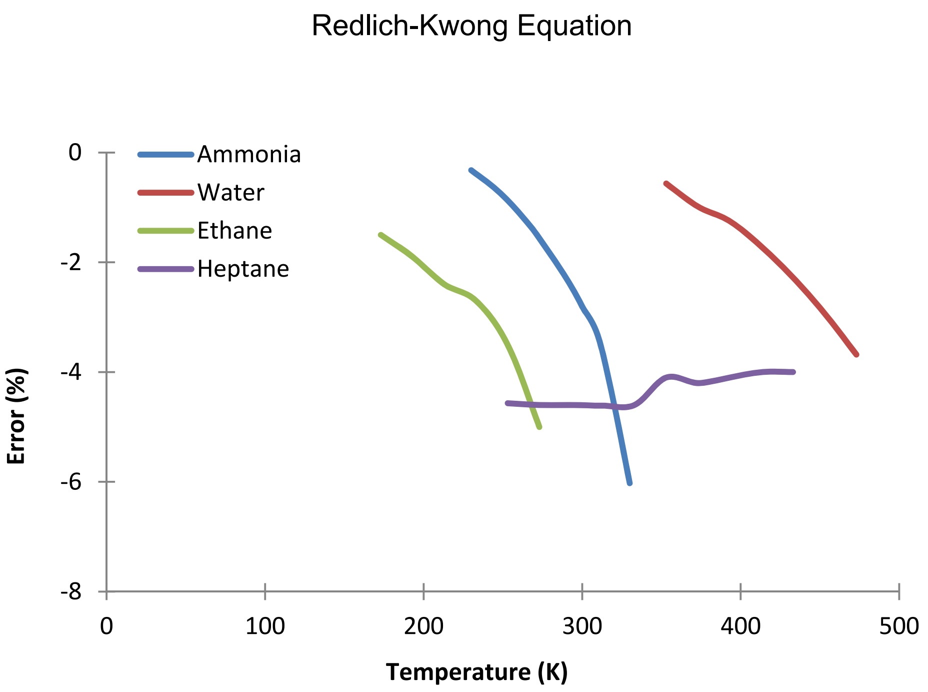

Figure 18: Redlich-Kwong Error

Inputs Required

- Critical Parameters: Pressure, Temperature, Volume

Types of compound		Temperature range (Reduced Temperature T_r)	Expected error (average)
Polar	Organic	$0.4 \leq T_r \leq 0.9$	$\% \leq 30$
	Inorganic	$0.4 \leq T_r \leq 0.9$	$0 \leq \% \leq 6$
Nonpolar		$0.4 \leq T_r \leq 0.9$	$0 \leq \% \leq 5$

Table 15: Redlich-Kwong equation parameter table

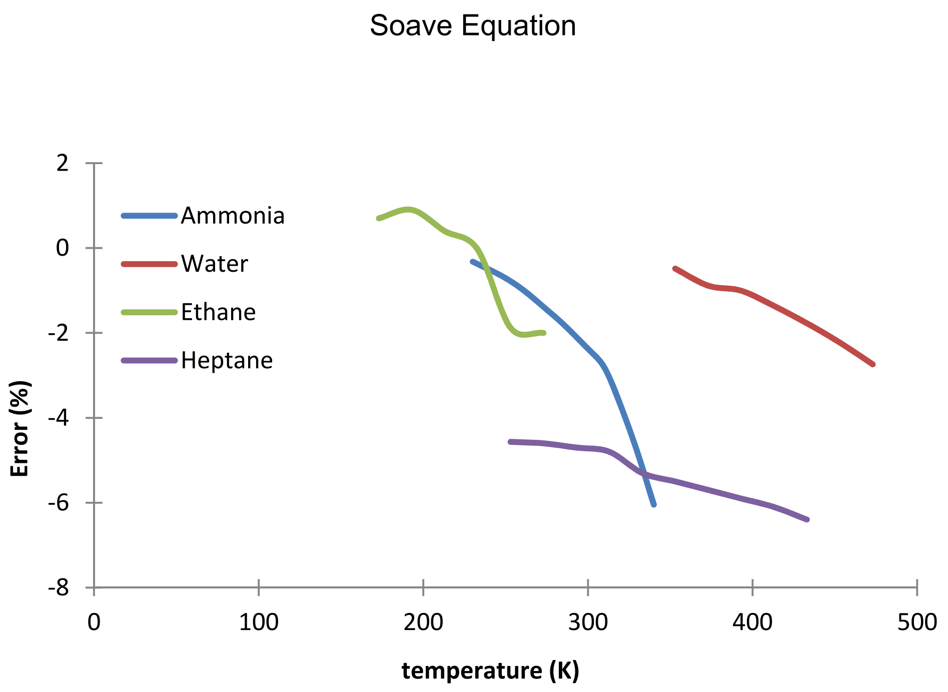

Figure 19: Soave Error

Inputs Required

- Critical Parameters: Pressure, Temperature, Volume
- Acentric Factor.

Types of compound		Temperature range (Reduced Temperature T_r)	Expected error (average)
Polar	Organic	$0.4 \le T_r \le 0.9$	$\% \le 20$
	Inorganic	$0.4 \le T_r \le 0.9$	$0 \le \% \le 6$
Nonpolar		$0.4 \le T_r \le 0.9$	$0 \le \% \le 5$

Table 16: Soave equation parameter table

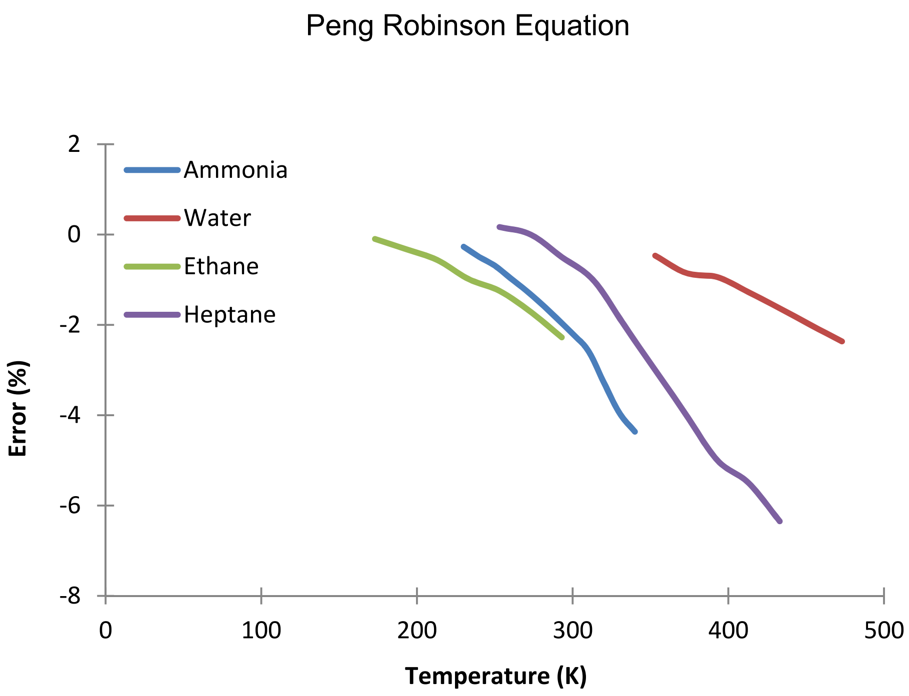

Figure 20: Peng-Robinson equation error

Inputs Required

- Critical Parameters: Pressure, Temperature, Volume
- Acentric Factor.

Types of compound		Temperature range (Reduced Temperature T_r)	Expected error (average)
Polar	Organic	$0.4 \leq T_r \leq 0.9$	$\% \leq 25$
	Inorganic	$0.4 \leq T_r \leq 0.9$	$0 \leq \% \leq 5$
Nonpolar		$0.4 \leq T_r \leq 0.9$	$0 \leq \% \leq 6$

Table 17: Peng-Robinson equation parameter table

Surface Tension

Macleod-Sudgen Equation

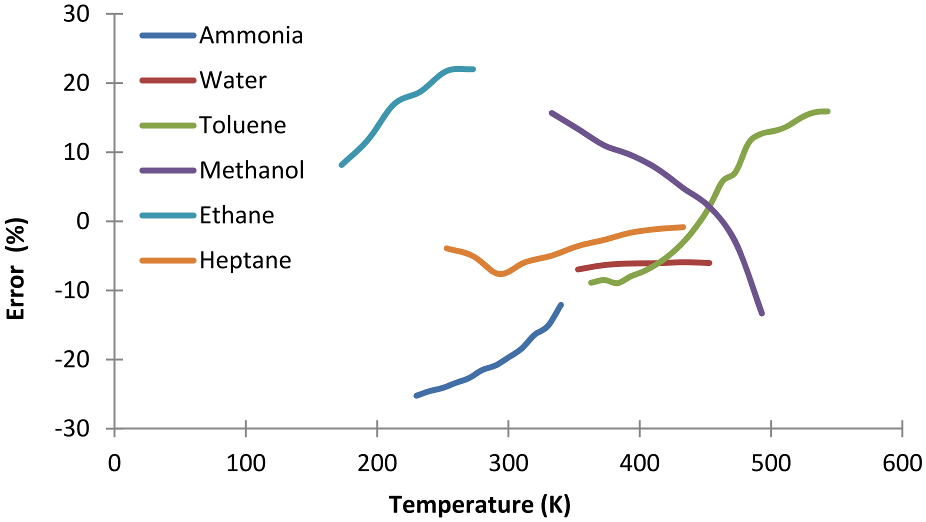

Figure 21: Macleod-Sudgen equation error

Inputs Required

- Molecular Structure
- Liquid Density & Vapor Density
- Molecular Weight

Types of compound		Temperature range (Reduced Temperature T_r)	Expected error (average)
Polar	Organic	$0.3 \leq T_r \leq 0.8$	$0 \leq \% \leq 20$
	Inorganic	$0.3 \leq T_r \leq 0.8$	$0 \leq \% \leq 25$
Nonpolar		$0.3 \leq T_r \leq 0.8$	$0 \leq \% \leq 20$

Table 18: Macleod-Sudgen equation parameter table

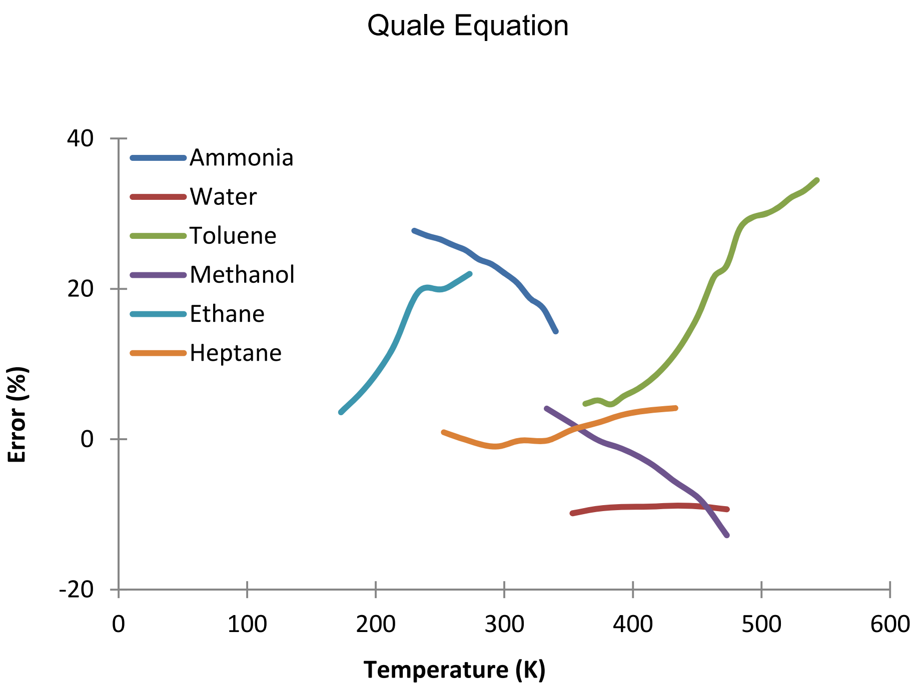

Figure 22: Quale equation error

Inputs Required

- Molecular Structure
- Liquid Density & Vapor Density
- Molecular Weight

Types of compound		Temperature range (Reduced Temperature T_r)	Expected error (average)
Polar	Organic	$0.3 \leq T_r \leq 0.9$	$0 \leq \% \leq 35$
	Inorganic	$0.3 \leq T_r \leq 0.9$	$0 \leq \% \leq 30$
Nonpolar		$0.3 \leq T_r \leq 0.9$	$0 \leq \% \leq 20$

Table 19: Quale equation parameter table

Brook's et al. Equation

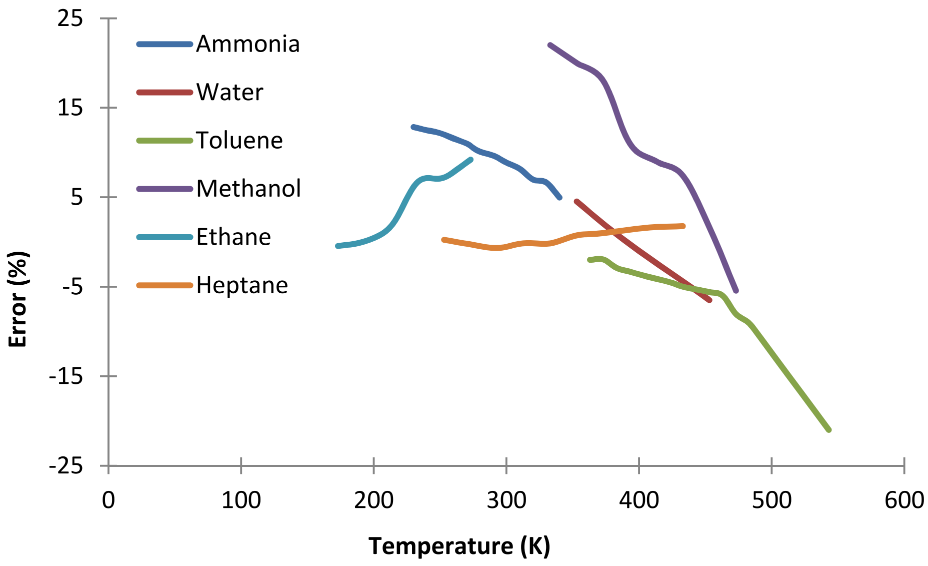

Figure 23: Brook's et al. equation error

Inputs Required

- Critical Parameters: Temperature, Pressure
- Boiling Temperature

Types of compound		Temperature range (Reduced Temperature T_r)	Expected error (average)
Polar	Organic	$0.3 \leq T_r \leq 0.9$	$0 \leq \% \leq 20$
	Inorganic	$0.3 \leq T_r \leq 0.9$	$0 \leq \% \leq 15$
Nonpolar		$0.3 \leq T_r \leq 0.9$	$0 \leq \% \leq 10$

Table 20: Brook's et al. equation parameter table

Liquid Viscosity

Vogel Equation

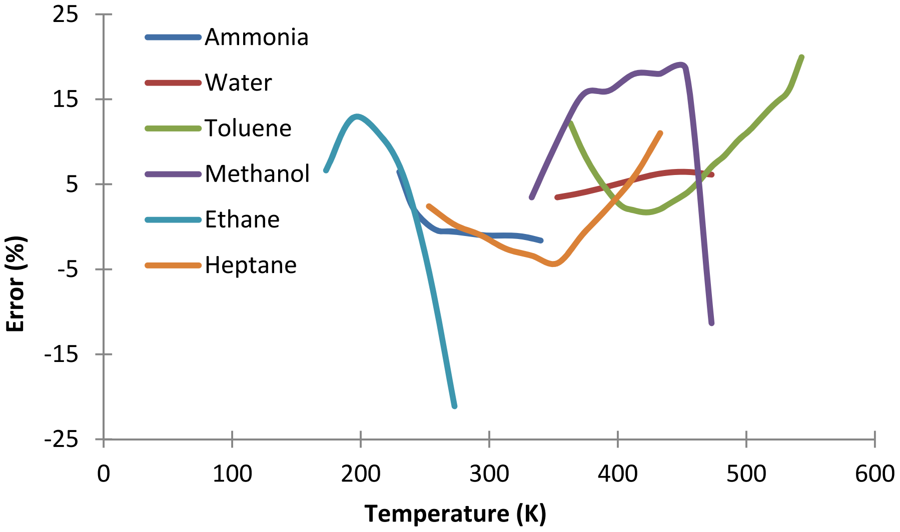

Figure 24: Vogel Equation error

Inputs Required

- Vogel or Antoine Constants
- Critical Parameters: Temperature

Types of compound		Temperature range (Reduced Temperature T_r)	Expected error (average)
Polar	Organic	$0.3 \leq T_r \leq 0.9$	$0 \leq \% \leq 20$
	Inorganic	$0.3 \leq T_r \leq 0.9$	$0 \leq \% \leq 15$
Nonpolar		$0.3 \leq T_r \leq 0.9$	$0 \leq \% \leq 10$

Table 21: Vogel equation parameter table

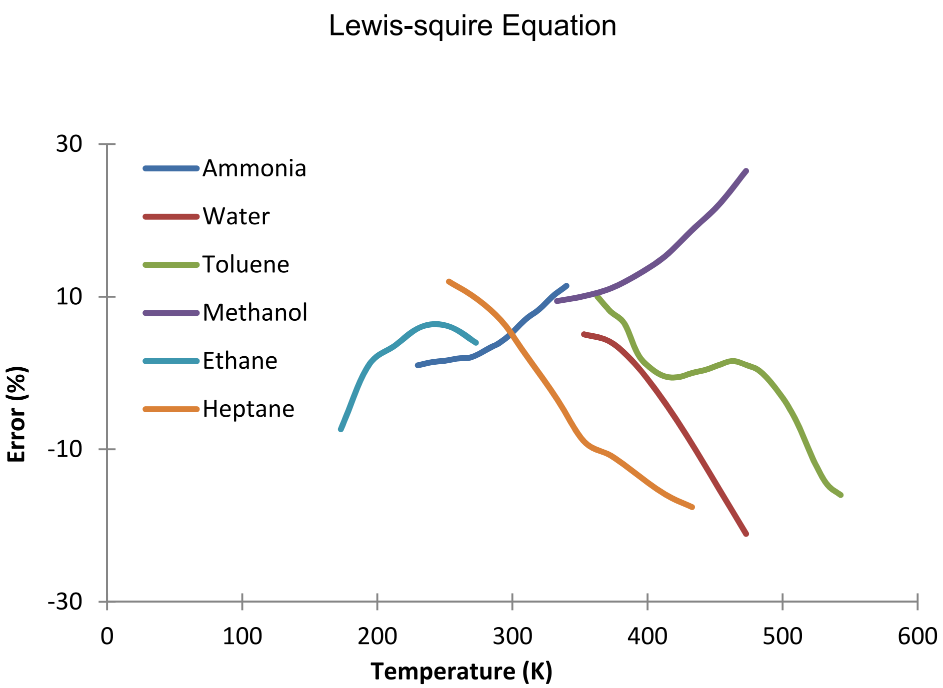

Figure 25: Lewis-Squire equation error

Inputs Required

- Critical Parameters: Temperature, Pressure
- Liquid viscosity at a known point.

Types of compound		Temperature range (Reduced Temperature T_r)	Expected error (average)
Polar	Organic	$0.3 \leq T_r \leq 0.9$	$0 \leq \% \leq 20$
	Inorganic	$0.3 \leq T_r \leq 0.9$	$0 \leq \% \leq 20$
Nonpolar		$0.3 \leq T_r \leq 0.9$	$0 \leq \% \leq 10$

Table 22: Lewis-Squire equation parameter table

Vapor Viscosity

Chung Equation

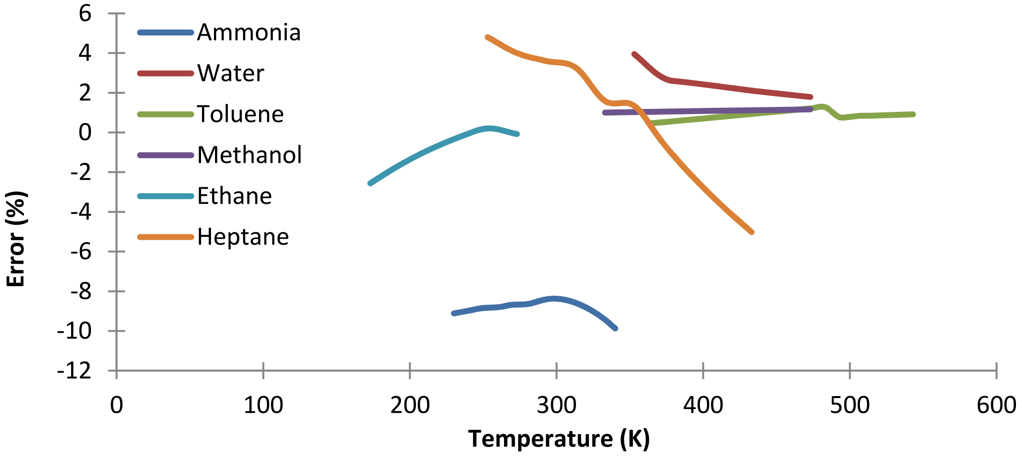

Figure 26: Chung equation error

Inputs Required

- Critical Parameters: Temperature, Pressure, Volume
- Molar weight
- Acentric Factor
- Dipole moment (Debye)

Types of compound		Temperature range (Reduced Temperature T_r)	Expected error (average)
Polar	Organic	$0.3 \leq T_r \leq 0.9$	$0 \leq \% \leq 2$
	Inorganic	$0.3 \leq T_r \leq 0.9$	$0 \leq \% \leq 10$
Nonpolar		$0.3 \leq T_r \leq 0.9$	$0 \leq \% \leq 5$

Table 23: Chung equation parameter table

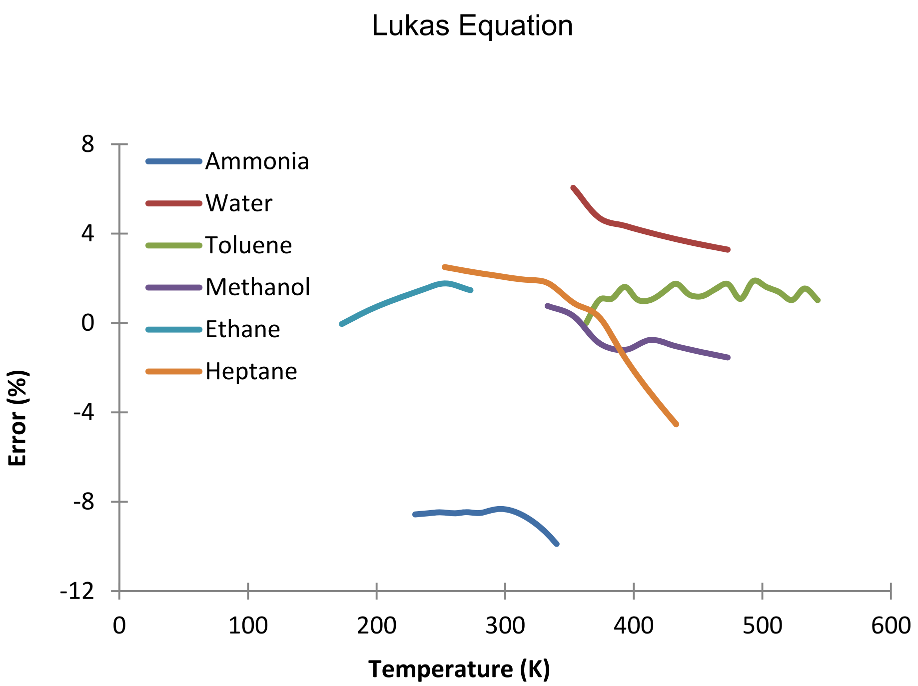

Figure 27: Lukas equation error

Inputs Required

- Critical Parameters: Temperature, Pressure, Volume, Compressibility Factor
- Dipole moment (Debye)
- Molar weight

Types of compound		Temperature range (Reduced Temperature T_r)	Expected error (average)
Polar	Organic	$0.3 \le T_r \le 0.9$	$0 \le \% \le 2$
	Inorganic	$0.3 \le T_r \le 0.9$	$0 \le \% \le 10$
Nonpolar		$0.3 \le T_r \le 0.9$	$0 \le \% \le 4$

Table 24: Lukas equation parametric table

<u>Merit Number</u>

The theory of uncertainty using standard deviation as the mode of tolerance was first used to calculate the percentage deviation of the important thermo-physical properties for all of the four considered working fluid. Every thermo-physical property in the working temperature range was expressed in the form of $\mathrm{x} = \mathrm{x}_{\mathrm{mean}} + \mathrm{s.d}$, where s.d is the standard deviation about the mean at the given temperature. The percent deviation of the liquid and the vapor merit number is shown in Eq. 52.The standard deviation for the liquid merit number is shown in Fig. 28 and that of vapor in Fig. 29.

$$\frac{\Delta F.m_{l,v}}{F.m_{l,v}} = \left(\sqrt[2]{\left(\frac{s.d\,(\rho)}{\rho_{mean}}\right)^2 + \left(\frac{s.d\,(\mu)}{\mu_{mean}}\right)^2 + \left(\frac{s.d\,(\sigma)}{\sigma_{mean}}\right)^2 + \left(\frac{s.d\,(\lambda)}{\lambda_{mean}}\right)^2}\right)_{l,v} \qquad (52)$$

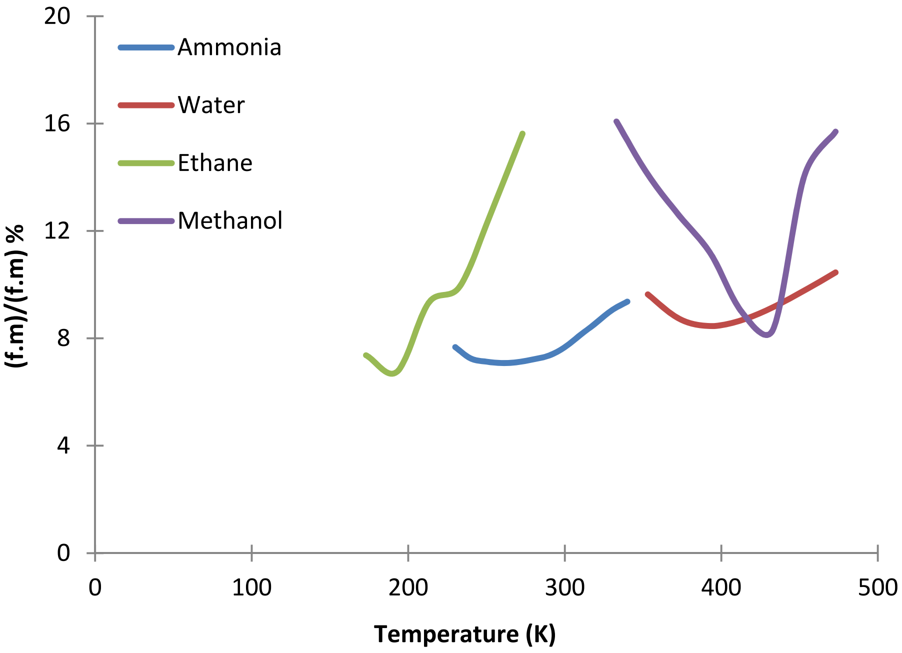

Figure 28: Liquid merit number uncertainty (standard deviation)

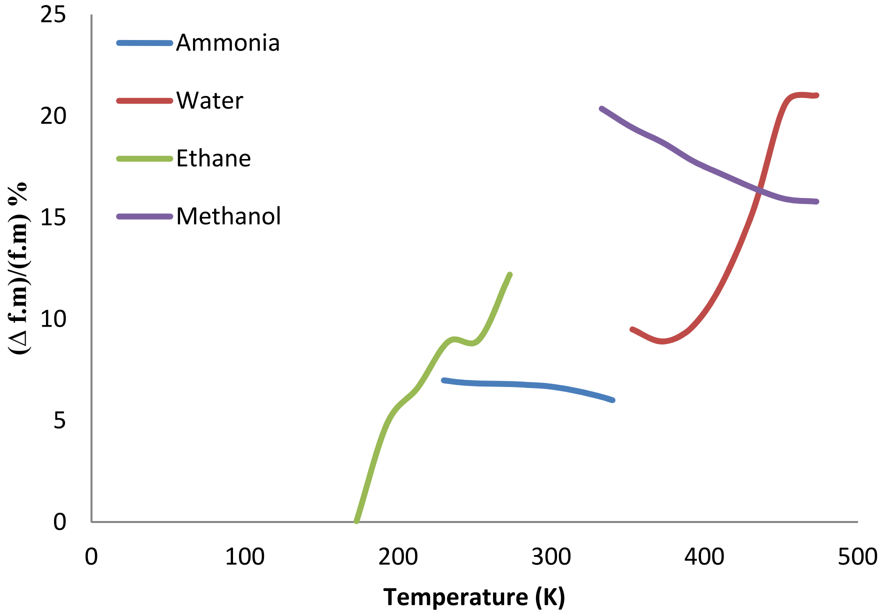

Figure 29: Vapor merit number uncertainty (standard deviation)

The Fig. 28 and Fig. 29 shows that the standard deviation for liquid and vapor merit number is not more than 20% for any fluid.. The x_{mean} for every property was used to determine the calculative merit number for all the four fluids (ammonia, water, ethane and methanol). Hence it can be inferred that the mean or average value of the thermo-physical property can be used to calculate the theoretical merit number and compare it with the experimental merit number for determining the feasibility for use in main systems. The Eq. 53 gives the percentage error equation in vapor and liquid merit number. Fig. 30 and Fig. 31 shows the error in liquid merit number and vapor merit number respectively.

$$(\mathrm{f.m})_{\mathrm{liquid,vapor}}\ \%\ \mathrm{Error}\left(\frac{\left(\frac{\rho*\lambda*\sigma}{\mu}\right)_{\mathrm{mean}}-\mathrm{f.m}_{\mathrm{experimental}}}{\mathrm{f.m}_{\mathrm{experimental}}}\right)_{\mathrm{liquid,vapor}} * 100 \qquad (53)$$

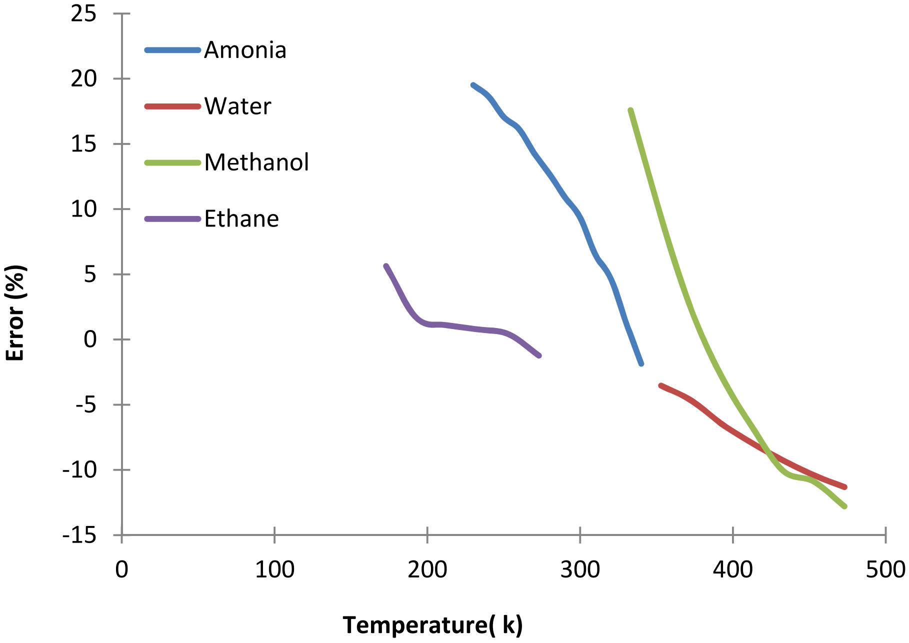

Figure 30: Liquid Merit number error

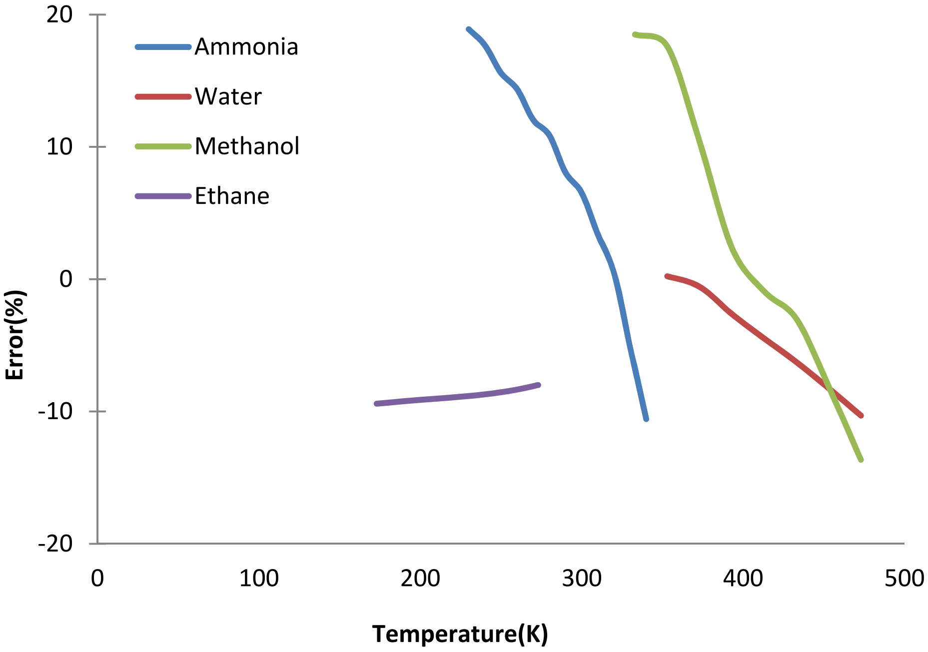

Figure 31: Vapor Merit number Error

Maximum Heat Transfer

In the literature review, it was discussed through Eq. (6) that the maximum heat carrying capacity of the cylindrical liquid pressure driven heat pipe depends on three factors i.e. the thermo-physical properties of the fluid, the wick properties and geometrical design of the heat pipe. In this work, the fluid selection was only considered for performance optimization in this work, for which maximum heat transfer capability is a key concept to evaluate. For considering the maximum heat carrying capacity which directly reflects the effectiveness of the heat pipe an uncertainty analysis was done on the Eq. (6) considering 5% uncertainty in geometric design of the heat pipe.

$$\frac{\Delta Q_m}{Q_m} = \left(\sqrt[2]{\left(\frac{\Delta F.m_l}{F.m_l}\right)^2 + \left(\frac{\Delta\, Wick\ Properties}{Wick\ Properties}\right)^2 + \left(\frac{\Delta Design}{Design}\right)^2} \right)_{l,v} \tag{54}$$

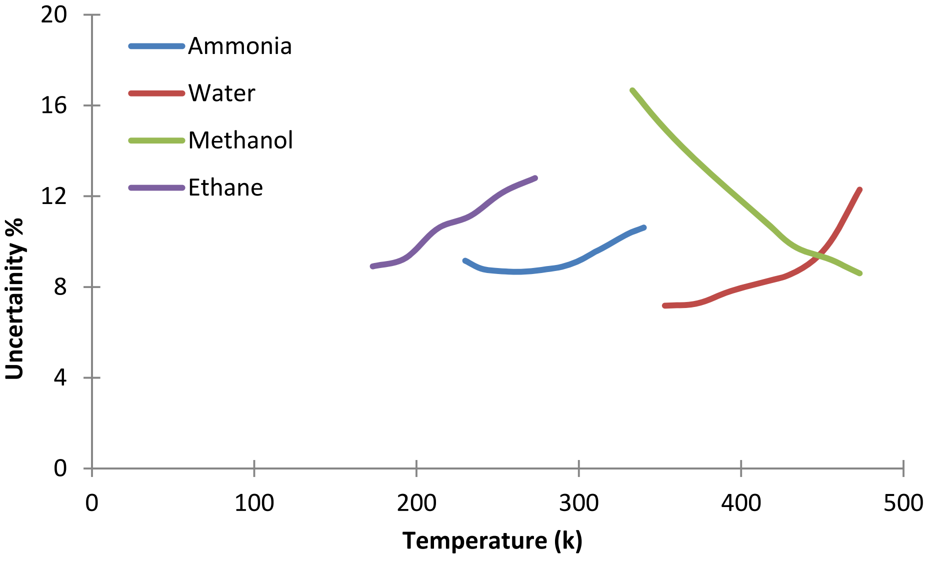

Figure 32: Maximum heat transfer error percentage

For working fluids ammonia, ethane and methanol, Fig. 33 to 35 show the maximum heat transport capacity "Q_m" (W) calculated from the experimental data available [43], the mean heat transport capacity calculated by the methods used and the error it produces at every temperature. Once again it was found that for the entire operating temperature the error percentage does not exceed 20%, which is an acceptable approximation for an engineering calculation. Altogether, Q_m was calculated for every fluid (Ammonia, water, ethane and methanol). In the same figure at every temperature the error between the experimental and formulated average value was plotted to demonstrate the rate of difference between the two values. The geometric specification mentioned for calculations (for conventional heat pipe) are:

Outer diameter	0.005 m.
Length	0.1 m.
Wick porosity	0.75.
Capillary radius	10^{-5} m.

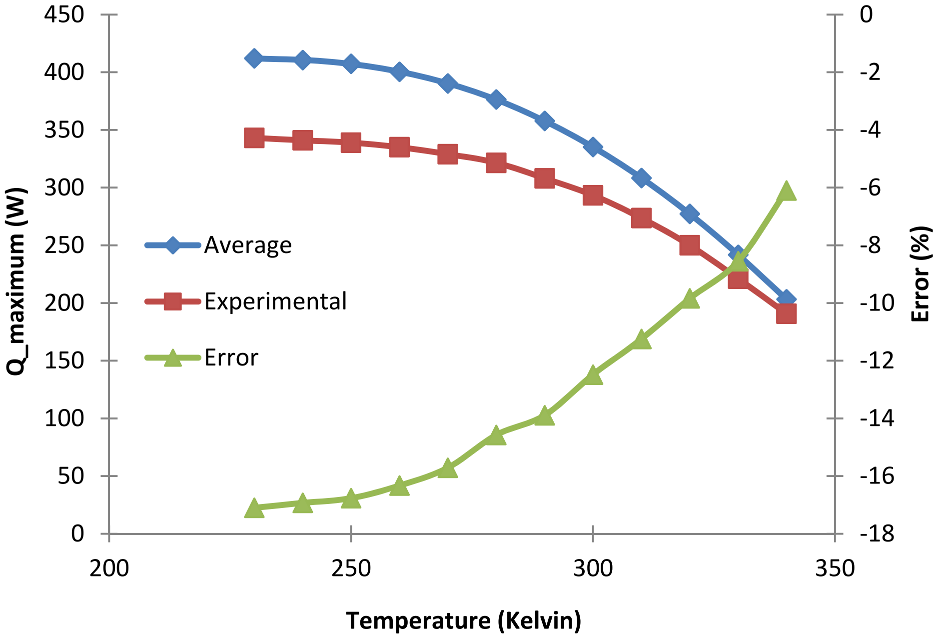

Figure 33: Ammonia Q_{max} with error

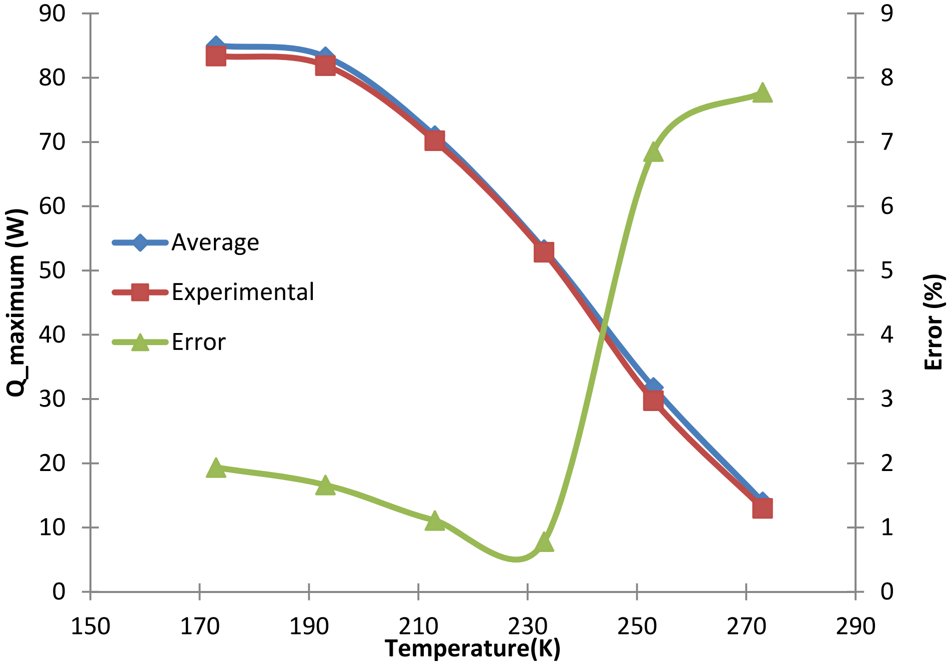

Figure 34: Ethane Q_{max} with error

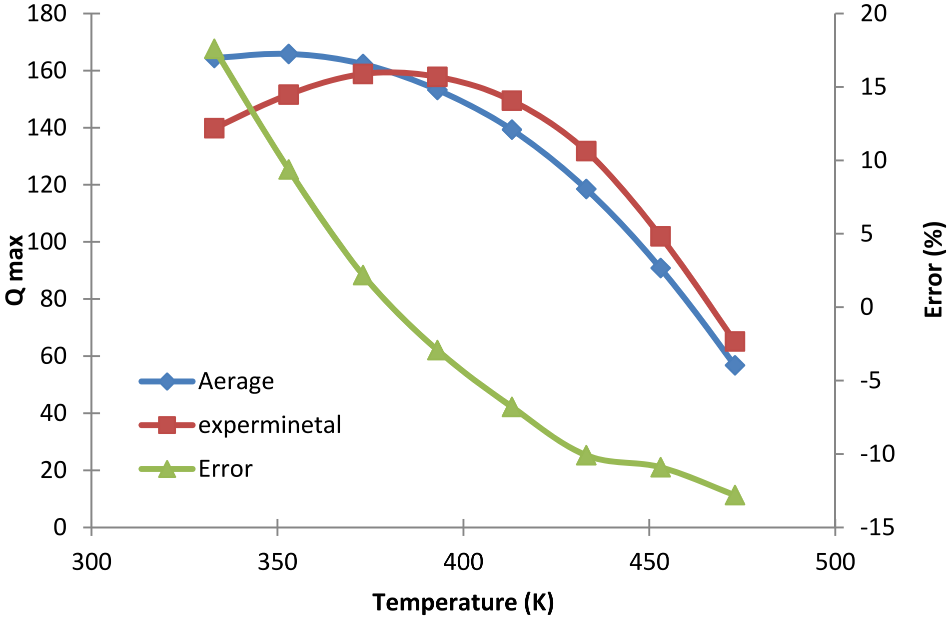

Figure 35: Methanol Qmax with error

Discussion

Latent Heat of vaporization

Pitzer’s three state parameter equation works well with organic fluids, whereas the Watson’s correlation linked with either Viswanath or Riedel is found to work with nonpolar fluids.

Fluid Type		Recommended Method	Error (%)
Polar	Organic	Pitzer [22]	$0 \leq \% \leq 3$
	Inorganic	Watson-Viswanath[38,40]	$0 \leq \% \leq 4$
Nonpolar		Watson-Riedel [37,40]	$0 \leq \% \leq 2$

Table 25: Latent Heat Recommendation

Liquid Density

Although the Francis method for formulating the liquid density as a function of temperature holds accurate for the entire range of temperature, but for determining the Francis constants it is recommended to consult his work.

Fluid Type		Recommended Method	Error (%)
Polar	Organic	Yen & woods [29]	$0 \leq \% \leq 3$
	Inorganic	Gunn & Yamada [32]	$0 \leq \% \leq 3$
Nonpolar		Yen & woods [29]	$0 \leq \% \leq 3$

Table 26: Liquid Density recommendation

Vapor Density

The error for formulating the vapor density decreases as we go down with methods described in table 4. However, the error given by the methods for polar organic compounds (methanol) was high enough for not considering it as the method of evaluation.

Fluid Type		Recommended Method	Error (%)
Polar	Organic	Peng-Robinson[19]	
	Inorganic	Peng-Robinson [19]	$0 \leq \% \leq 5$
Nonpolar		Soave [19]	$0 \leq \% \leq 5$

Table 27: Vapor Density recommendation

Surface Tension

Macleod and Sudgen's correlation form the base of all methods leading to the formulation of surface tension as a function of temperature, but are often encountered with high errors.

Fluid Type		Recommended Method	Error (%)
Polar	Organic	Brooks et al. [37]	$0 \leq \% \leq 20$
	Inorganic	Brooks et al. [37]	$0 \leq \% \leq 15$
Nonpolar		Brooks et al. [37]	$0 \leq \% \leq 10$

Table 28: Surface Tension Recommendation

Liquid Viscosity

The Vogel equation was the first equation expressing the inverse exponential nature of the liquid viscosity, however considerable work has been done in the form Lewis-Squire correlation to formulate it as a function of temperature.

Fluid Type		Recommended Method	Error (%)
Polar	Organic	Lewis-Squire [14]	$0 \leq \% \leq 20$
	Inorganic	Vogel [14]	$0 \leq \% \leq 15$
Nonpolar		Lewis-Squire [14]	$0 \leq \% \leq 10$

Table 29: Liquid Viscosity Recommendation

Vapor Viscosity

As quoted by Dunbar and Cadell, surface tension and viscosity are the least documented property for temperature formulation. But, some work has been done to formulate both as a function of temperature.

Fluid Type		Recommended Method	Error (%)
Polar	Organic	Lukas [14]	$0 \leq \% \leq 2$
	Inorganic	Cheng [36] & Lukas [14]	$0 \leq \% \leq 10$
Nonpolar		Lukas [14]	$0 \leq \% \leq 4$

Table 30: Vapor Viscosity Recommendation

CHAPTER 4

CONCLUSION

Four thermal fluids ammonia, water, ethane and methanol were selected for model formulation in order to consider various methods for evaluation of the liquid and vapor merit number in a conventional heat pipe. The evaluation criteria were based upon calculating the error percent with the reference data and determining the uncertainty deviation about the mean. Thereafter, the analysis was continued on maximum heat transfer capacity of the working fluid.

For considering the calculation of merit number, irrespective of it being a vapor or a liquid merit number, the most important thermo-physical properties of interest are latent heat of vaporization, density (liquid and vapor), surface tension, viscosity(liquid and vapor) and vapor pressure. This work formulates vapor pressure so as to have an idea of the operating temperature range of the thermal fluid.

Latent heat of vaporization has several unique methods of formulation using only the intensive properties of the thermal fluid. Pitzer equation is considered to work well for polar fluids, whereas Watson-Riedel equation works well for nonpolar fluids. The maximum error using any method was 8% and the minimum was 2% using the recommended methods.

Liquid density, reports a minimum error of 3% using Yen & Woods equation for polar organic fluid and nonpolar fluid, whereas Gunn & Yamada equation for polar inorganic fluids. The maximum error reports for liquid density is 7%. Since vapor density gives higher errors when compared to liquid density, it is recommended to not be used for polar organic fluids. When using Peng-Robinson equation, the minimum error was calculated as 5 % whereas, the maximum error was calculated as 25%.

Brook’s equation, using the critical parameters for surface tension formulation reports the minimum error of 10% for nonpolar fluids and 15-20% error for polar compounds. Macleod’s correlation accounts for approximately 25% error for all fluids.

Using Lewis-squire equation, 10% and 15% error was calculated in nonpolar and polar fluids respectively. A maximum of 20% error was calculated for polar fluids using vogel equation. An average of 2% error was calculated in polar organic fluids by using Chung equation and Lukas equation, whereas a 5% error was seen in non-polar fluids.

Polar inorganic fluid like ammonia and water exhibits 10% standard deviation in liquid and vapor merit number for the conventional heat pipe. The maximum heat transport capability of ammonia and water accounts for a maximum of 20% error which improves to a minimum of 6% at 340 K for ammonia and 5% at 450 K for water.

Methanol, a polar organic thermal fluid accounts for a maximum of 15% standard deviation for liquid and vapor merit number. The maximum heat transport capability of methanol is calculated as 15% at the extreme ends of the working temperature.

Ethane, a nonpolar organic fluid accounts for 15% standard deviation for liquid and vapor merit number. The maximum heat transport capability of ethanol is calculated to be a maximum of 8%.

CHAPTER 5

RECOMMENDATIONS FOR FUTURE WORK

- Liquid density has been formulated perfectly over the entire temperature range and does not require any further work.
- New methods for formulating vapor density for polar organic fluids are needed. There has been some work in formulating critical compressibility factor as a function of reduced temperature which can be helpful.
- Introduction of acentric factor in latent heat of vaporization calculation in Watson methods may decrease the error even further.
- Some work can be done in reducing the error in surface tension and liquid density to 5-10%. All methods described accounts for a minimum of 15% error.
- The analysis should be extended to more fluids to validate the results.
- As we have not considered any fluid (whether polar or nonpolar) over 500 K, So further study of temperature above 500 K is needed to validate the study.
- Work on metal fluids (in molten states) from 800 K to 1500 K should be extended with the most potential candidates as lithium, cesium and sodium.
- This work is related to heat transport calculation of only liquid pressure gradient driven heat pipe, but there have been theories which relate vapor as well as gravity pressure gradient driven heat pipes. Such theories should also be validated.

APPENDICES

Appendix A: Lyckman et al. [30] Generalized reduced temperature parameters

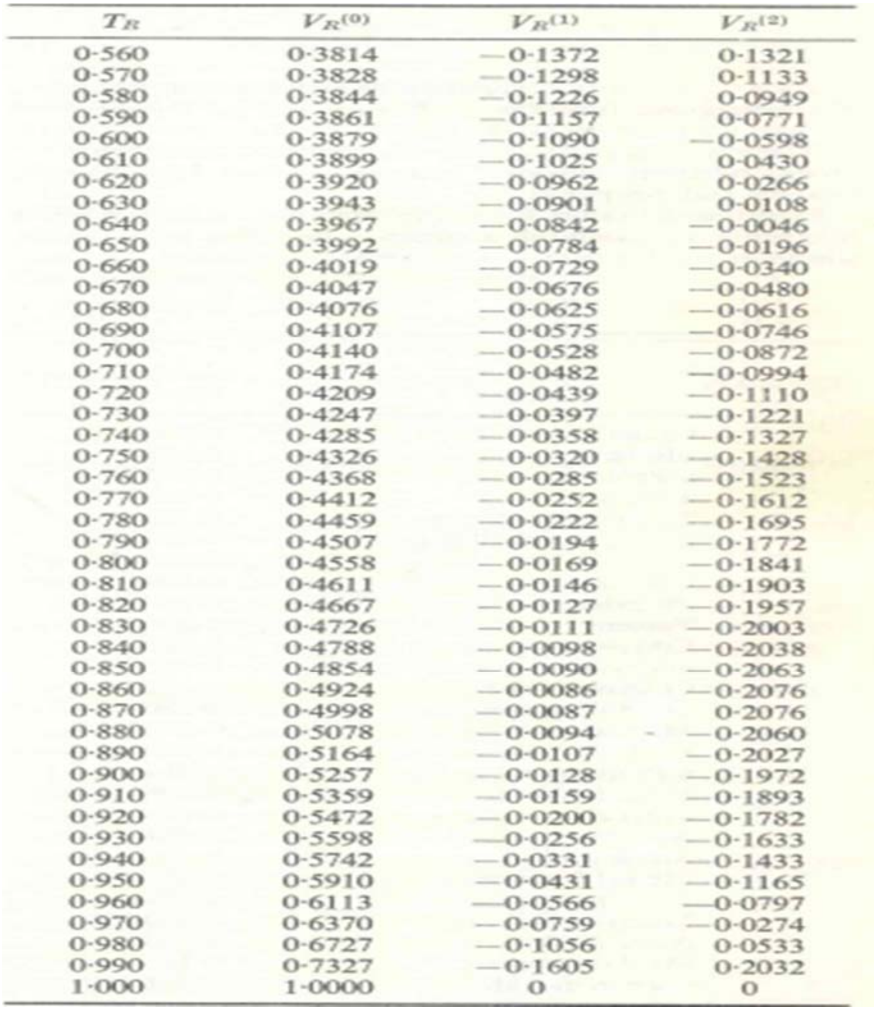

T_R	$V_R^{(0)}$	$V_R^{(1)}$	$V_R^{(2)}$
0·560	0·3814	—0·1372	0·1321
0·570	0·3828	—0·1298	0·1133
0·580	0·3844	—0·1226	0·0949
0·590	0·3861	—0·1157	0·0771
0·600	0·3879	—0·1090	—0·0598
0·610	0·3899	—0·1025	0·0430
0·620	0·3920	—0·0962	0·0266
0·630	0·3943	—0·0901	0·0108
0·640	0·3967	—0·0842	—0·0046
0·650	0·3992	—0·0784	—0·0196
0·660	0·4019	—0·0729	—0·0340
0·670	0·4047	—0·0676	—0·0480
0·680	0·4076	—0·0625	—0·0616
0·690	0·4107	—0·0575	—0·0746
0·700	0·4140	—0·0528	—0·0872
0·710	0·4174	—0·0482	—0·0994
0·720	0·4209	—0·0439	—0·1110
0·730	0·4247	—0·0397	—0·1221
0·740	0·4285	—0·0358	—0·1327
0·750	0·4326	—0·0320	—0·1428
0·760	0·4368	—0·0285	—0·1523
0·770	0·4412	—0·0252	—0·1612
0·780	0·4459	—0·0222	—0·1695
0·790	0·4507	—0·0194	—0·1772
0·800	0·4558	—0·0169	—0·1841
0·810	0·4611	—0·0146	—0·1903
0·820	0·4667	—0·0127	—0·1957
0·830	0·4726	—0·0111	—0·2003
0·840	0·4788	—0·0098	—0·2038
0·850	0·4854	—0·0090	—0·2063
0·860	0·4924	—0·0086	—0·2076
0·870	0·4998	—0·0087	0·2076
0·880	0·5078	—0·0094	—0·2060
0·890	0·5164	—0·0107	—0·2027
0·900	0·5257	—0·0128	—0·1972
0·910	0·5359	—0·0159	—0·1893
0·920	0·5472	—0·0200	—0·1782
0·930	0·5598	—0·0256	—0·1633
0·940	0·5742	—0·0331	—0·1433
0·950	0·5910	—0·0431	—0·1165
0·960	0·6113	—0·0566	—0·0797
0·970	0·6370	—0·0759	—0·0274
0·980	0·6727	—0·1056	0·0533
0·990	0·7327	—0·1605	0·2032
1·000	1·0000	0	0

Appendix B: Scaling Volume and Critical Volume for Gunn et al. [32]

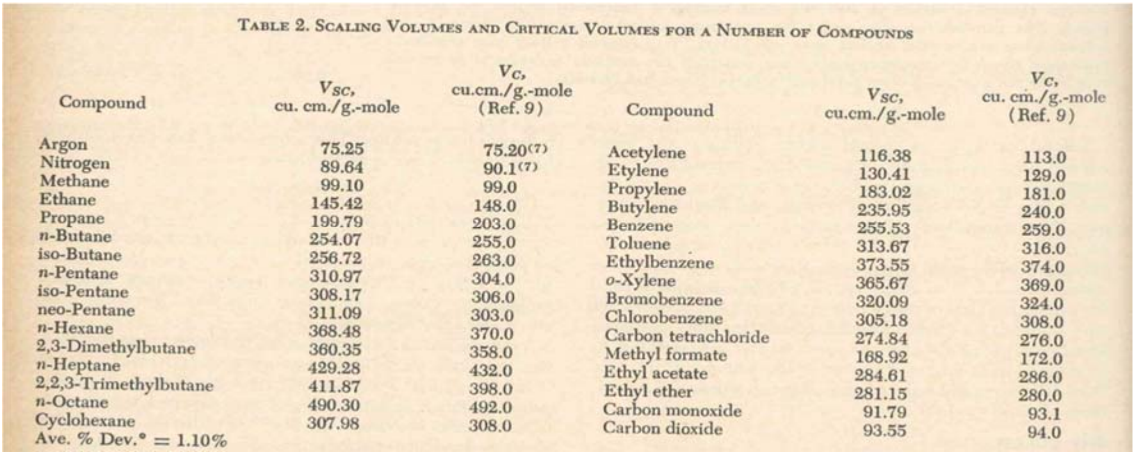

TABLE 2. SCALING VOLUMES AND CRITICAL VOLUMES FOR A NUMBER OF COMPOUNDS

Compound	V_{SC}, cu. cm./g.-mole	V_C, cu.cm./g.-mole (Ref. 9)	Compound	V_{SC}, cu.cm./g.-mole	V_C, cu. cm./g.-mole (Ref. 9)
Argon	75.25	75.20(7)	Acetylene	116.38	113.0
Nitrogen	89.64	90.1(7)	Etylene	130.41	129.0
Methane	99.10	99.0	Propylene	183.02	181.0
Ethane	145.42	148.0	Butylene	235.95	240.0
Propane	199.79	203.0	Benzene	255.53	259.0
n-Butane	254.07	255.0	Toluene	313.67	316.0
iso-Butane	256.72	263.0	Ethylbenzene	373.55	374.0
n-Pentane	310.97	304.0	*o*-Xylene	365.67	369.0
iso-Pentane	308.17	306.0	Bromobenzene	320.09	324.0
neo-Pentane	311.09	303.0	Chlorobenzene	305.18	308.0
n-Hexane	368.48	370.0	Carbon tetrachloride	274.84	276.0
2,3-Dimethylbutane	360.35	358.0	Methyl formate	168.92	172.0
n-Heptane	429.28	432.0	Ethyl acetate	284.61	286.0
2,2,3-Trimethylbutane	411.87	398.0	Ethyl ether	281.15	280.0
n-Octane	490.30	492.0	Carbon monoxide	91.79	93.1
Cyclohexane	307.98	308.0	Carbon dioxide	93.55	94.0

Ave. % Dev.* = 1.10%

Appendix C: Sudgen [18] atomic and Parachor values

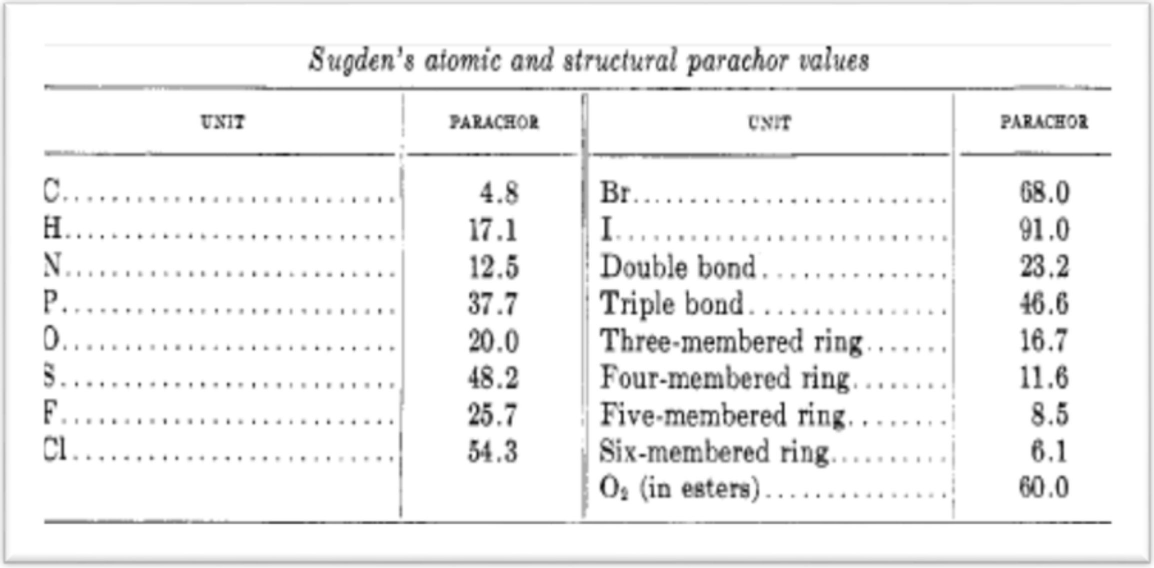

Sugden's atomic and structural parachor values

UNIT	PARACHOR	UNIT	PARACHOR
C	4.8	Br	68.0
H	17.1	I	91.0
N	12.5	Double bond	23.2
P	37.7	Triple bond	46.6
O	20.0	Three-membered ring	16.7
S	48.2	Four-membered ring	11.6
F	25.7	Five-membered ring	8.5
Cl	54.3	Six-membered ring	6.1
		O_2 (in esters)	60.0

Appendix D: Quale [21] Atomic and structural Parachor values

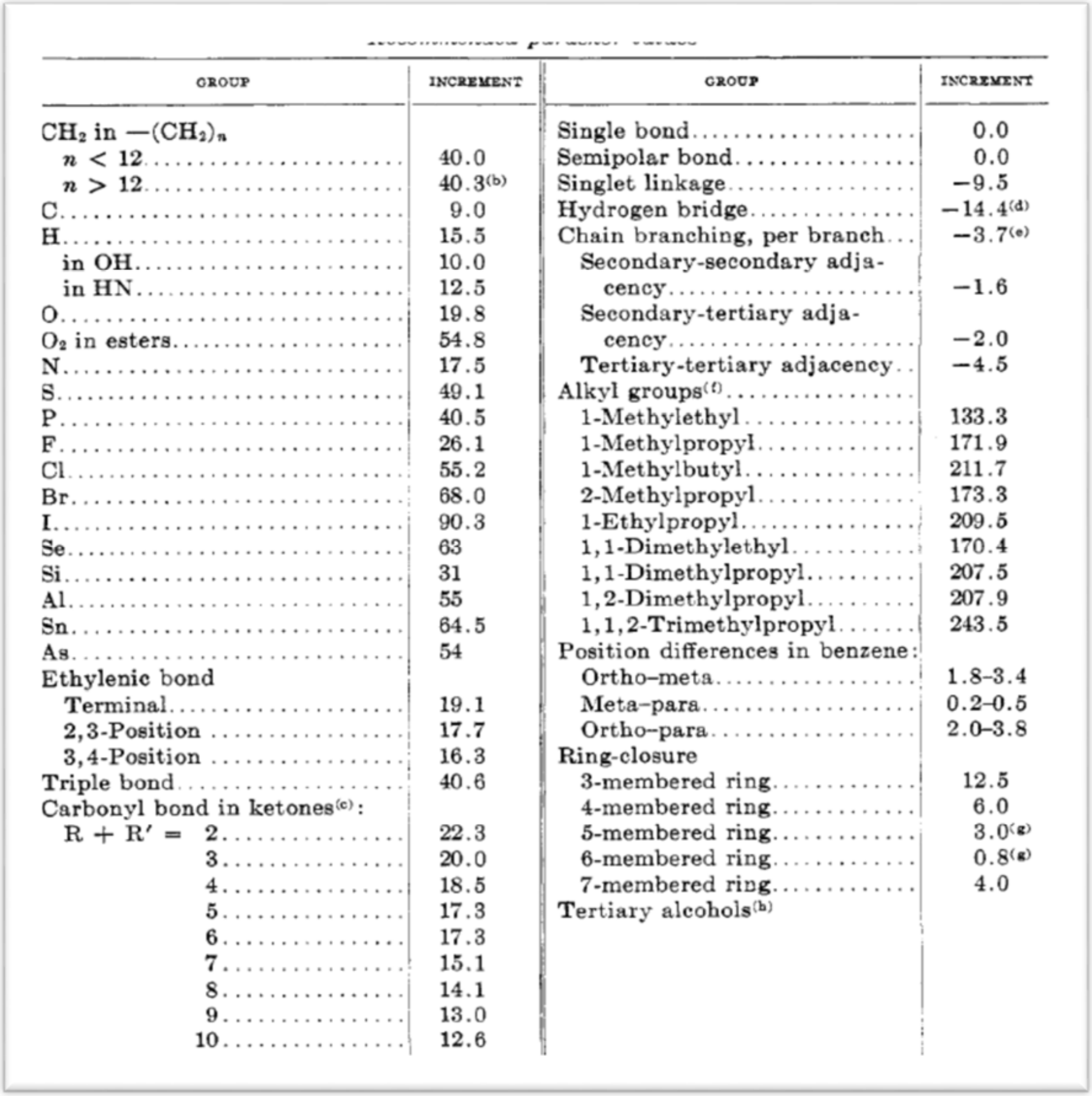

GROUP	INCREMENT
CH_2 in —$(CH_2)_n$	
$n < 12$	40.0
$n > 12$	40.3(b)
C	9.0
H	15.5
in OH	10.0
in HN	12.5
O	19.8
O_2 in esters	54.8
N	17.5
S	49.1
P	40.5
F	26.1
Cl	55.2
Br	68.0
I	90.3
Se	63
Si	31
Al	55
Sn	64.5
As	54
Ethylenic bond	
Terminal	19.1
2,3-Position	17.7
3,4-Position	16.3
Triple bond	40.6
Carbonyl bond in ketones(c):	
$R + R' = 2$	22.3
3	20.0
4	18.5
5	17.3
6	17.3
7	15.1
8	14.1
9	13.0
10	12.6
Single bond	0.0
Semipolar bond	0.0
Singlet linkage	−9.5
Hydrogen bridge	−14.4(d)
Chain branching, per branch	−3.7(e)
Secondary-secondary adjacency	−1.6
Secondary-tertiary adjacency	−2.0
Tertiary-tertiary adjacency	−4.5
Alkyl groups(f)	
1-Methylethyl	133.3
1-Methylpropyl	171.9
1-Methylbutyl	211.7
2-Methylpropyl	173.3
1-Ethylpropyl	209.5
1,1-Dimethylethyl	170.4
1,1-Dimethylpropyl	207.5
1,2-Dimethylpropyl	207.9
1,1,2-Trimethylpropyl	243.5
Position differences in benzene:	
Ortho–meta	1.8–3.4
Meta–para	0.2–0.5
Ortho–para	2.0–3.8
Ring-closure	
3-membered ring	12.5
4-membered ring	6.0
5-membered ring	3.0(g)
6-membered ring	0.8(g)
7-membered ring	4.0
Tertiary alcohols(h)	

Reference

1. Chi, S. W., Heat Pipe Theory and Practice a Sourcebook, McGraw-Hill, New York, 1976.

2. Long, J.B., “Alternate Working fluids for capillary driven two-phase loops”, MS Thesis, Clemson University, 2001.

3. Dunn, P.D., Reay, D.A., Heat Pipes, 2nd Ed., Pergamon Press, 1978.

4. Maydanik, Yu F. "Loop heat pipes." Applied Thermal Engineering 25.5: 635-657, 2005.

5. Ku, Kentung, "Operating characteristics of loop heat pipes. No. 1999-01-2007” SAE Technical Paper, 1999.

6. Launay, Stéphane, Valérie S., and Jocelyn B., "Parametric analysis of loop heat pipe operation: a literature review." International Journal of Thermal Sciences 46.7: 621-636, 2007.

7. Munson, B.R., Young, D.F., Fundamentals of fluid mechanics, 4th Ed., John Wiley & Sons, 2002.

8. Asselman, G.A.A., Green, D.B., “Heat Pipes. I. Operation and Characteristics”, Philips Technical Review, Vol. 33, Issue. 4, pp. 104-13, 1973.

9. Mishkinis, D., Ochterbeck, J.M., Sodtke, C., “Non-Dimensional Analysis and Scaling issues in Loop Heat Pipe”, 41s Aerospace Sciences Meeting and Exhibit, 6-9 Jan; Paper AIAA-2003-0341, 2003.

10. Dunbar, N. and Cadell, P., “Working Fluids and Figure of Merit for CPL/LHP Application”, The Aerospace Corporation, CPL-98 Workshop, 1998.

11. Wallin P, Heat Pipe Selection of working fluid, Project Report, MVK160 Heat and Mass Transfer, Lund, Sweden, 2012.

12. Chandratilleke, R., Hatakeyama, H., and Nakagome, H., "Development of cryogenic loop heat pipes." Cryogenics 38.3, 1998.

13. Deverall, J.E., “Mercury as a Heat Pipe Fluid”, ASME Paper 70-HT/Spt-8, 1970.

14. Anderson, W.G., Rosenfeld J.K., Angirasa, D., Mi,Y., “Evaluation of heat Pipe working fluid in the temperature range 450 to 700 K”, STAIF 2005, Albuquerque, NM, February 13-17, 2005.

15. Wei, Q., “Super High Temperature Heat Pipes”, Institute of Engineering, Chinese Academy of Science, Beijing, China.

16. Devarakonda, A., Anderson, W.G. , “Thermo-physical properties of intermediate temperature heat pipe fluids”, Space Technology & Applications International Forum (STAIF) Conference, vol. 746, American Institute of Physics, New York, 2005.

17. http://www.thermopedia.com/

18. Thomson, G. W., "The Antoine equation for vapor-pressure data”. Chemical reviews 38.1: 1-39, 1946.

19. Wagner, W. "New vapor pressure measurements for argon and nitrogen and a New method for establishing rational vapor pressure equation”, Cryogenics 13.8: 470-482, 1973.

20. Forero G, Luis A., and. Velásquez J. A., "Wagner liquid–vapor pressure equation constants from a simple methodology." The Journal of Chemical Thermodynamics 43.8: 1235-1251, 2011.

21. Pitzer, K.S., “The Volumetric and Thermodynamic Properties of fluids. II. Compressibility Factor, Vapor Pressure and Entropy of Vaporization 1”, Journal of the American Chemical Society 77.13: 3433-3440, 1950.

22. Lee, B.K. and Kesler, M.G., "A generalized thermodynamic correlation based on three-parameter corresponding states." AIChE Journal 21.3: 510-527, 1975.

23. Watson, K. M. "Thermodynamics of the liquid state." Industrial & Engineering Chemistry 35.4: 398-406, 1943.

24. Viswanath, D. S., and Kuloor, N. R., “On a generalized Watson's Relation for Latent heat of vaporization." The Canadian Journal of Chemical Engineering 45.1: 29-31, 1967.

25. Mehmandoust, B., Ehsan S., and Mostafa V., "An efficient reliable method to estimate the vaporization enthalpy of pure substances according to the normal boiling temperature and critical properties." Journal of Advanced Research 5.2: 261-269, 2014.

26. Chen, N. H. "Generalized Correlation for Latent Heat of Vaporization." Journal of Chemical and Engineering Data 10.2: 207-210, 1965.

27. Lyckman, E. W., Eckert, C. A. and Prausnitz, J. M. "Generalized liquid volumes and solubility parameters for regular solution application." Chemical Engineering Science 20.7: 703-706, 1965.

28. Francis, Alfred W. "Pressure-temperature-density relations of pure liquids", Chemical Engineering Science 10.1 (1959): 37-46.

29. Yen, Lewis C., and S. S. Woods. "A generalized equation for computer calculation of liquid densities." AIChE Journal 12.1: 95-99, 1966.

30. Riedel, L.,' Density of liquids in the state of saturation. Investigations on the widening of the theorem of corresponding states. II", Chemie ingenieur technik 20: 259-264, 1954.

31. Gunn, R. D., and Tomoyoshi Yamada. "A corresponding states correlation of saturated liquid volumes." AIChE Journal 17.6: 1341-1345, 1971.

32. Kenneth, W., Thermodynamics. New York: McGraw-Hill, 1977.

33. Poling, Bruce E., Prausnitz,J.M. and Reid, R. C., The properties of gases and liquids, 4th Ed., New York: McGraw-Hill, 1986.

34. Vargaftik, N. B., Volkov, B. N. and Voljak, L. D., "International tables of the surface tension of water." Journal of Physical and Chemical Reference Data 12.3: 817-820, 1983.

35. Vargaftik, N. B. "Handbook of thermo physical properties of gases and liquids." 1972.

36.Macleod, D. B. "On a relation between surface tension and density." Transactions of the Faraday Society 19.July: 38-41, 1923.

37. Sudgen, S. "VI.—the variation of surface tension with temperature and some related functions." Journal of the Chemical Society, Transactions 125: 32-41, 1924.
38. Quayle, O. R., "The Parachors of Organic Compounds. An Interpretation and Catalogue." Chemical Reviews 53.3: 439-589, 1953.

39. Brock, J. R. and Bird, R. B. "Surface tension and the principle of corresponding states." AIChE Journal 1.2: 174-177, 1955.

40. Neufeld, P. D., Janzen, A. R. and Aziz, R. A., "Empirical Equations to Calculate 16 of the Transport Collision Integrals Ω (l, s)* for the Lennard-Jones (12–6) Potential." The Journal of Chemical Physics 57.3:1100-1102, 2003.

41. Chung, T. H., Lloyd L. L. and Starling, K.E., "Applications of kinetic gas theories and multi-parameter correlation for prediction of dilute gas viscosity and thermal conductivity." Industrial & engineering chemistry fundamentals 23.1: 8-13, 1984.

42. Yoonm, P., and George T., "Viscosity of nonpolar gaseous mixtures at normal pressures." AIChE Journal 16.2: 300-304, 1970.